Relationship between fissility, composition, rock fabric and reservoir properties in Vaca Muerta Formation (Neuquén Basin, Argentina): from outcrop to subsurface core data

*Lucía Inés Martín[1], Denis Marchal[2], Silvia Barredo[1, 3],
Claudio Naides[2], Silvia Blanco Ibáñez[4]

[1] *Instituto Tecnológico de Buenos Aires (ITBA), Av. Madero 399, C1106 CABA, Argentina.*
lucmartin@itba.edu.ar

[2] *Pampa Energía S.A. Maipú 1, Piso 14, CABA, C1084ABA, Buenos Aires, Argentina.*
denis.marchal@pampaenergia.com; claudio.naides@pampaenergia.com.

[3] *Instituto del Gas y del Petróleo de la Universidad de Buenos Aires (IGPUBA), Av. Las Heras 2214 3P, CABA, Argentina.*
sbarredo@itba.edu.ar

[4] *LCV S.R.L. DE ARGENTINA, Parque Industrial Tecnológico Florencio Varela (PITEC), Calle 1236 No. 1238, Barrio La Carolina, Ruta Provincial 36, Km 34, Bosques (1888), Florencio Varela, Buenos Aires, Argentina.*
silviablanco@lcvsrl.com.ar

* Corresponding author: lucmartin@itba.edu.ar

ABSTRACT. The fissility is the ability of some rocks to split along relatively smooth surfaces parallel to the bedding. This property observed mostly in fine-grained rocks is particularly expressed in outcrops, where rocks are subjected to weathering processes. Most authors associate the fissility to the abundance of clay minerals and their orientation parallel to the bedding. The horizontal fabric can be promoted by depositional conditions such as sediment composition, quantity of total organic carbon content (TOC) and depositional mechanisms, giving rise to a primary fissility. Alternatively, the alignment of platy minerals can be linked to the burial history of the rock, by processes such as mechanical compaction or secondary mineral growth, resulting in a secondary fissility. The present study aims to identify the main controls of fissility development at the micro- and macroscopic scale in rocks of the Vaca Muerta Formation exposed in the Cerro Mulichinco area and in a 121-meter-long core extracted from a well within the Neuquén Basin. In outcrops, fissility is related to fine-grained laminated facies with low carbonate content, revealing the strong control exerted by lithology. The TOC measurements allow establishing a positive correlation between organic matter content and fissility intensity. Moreover, the analysis of the transgressive-regressive cycles shows that fissility is higher around the maximum flooding surfaces. Regarding their mechanical characteristics, the different interfaces observed in core are classified into first and second-order, the last one including fissility planes. Some of these interfaces evolve from potential (partially open) to effective (totally open) discontinuities in response to changes of stress conditions during the core extraction and due to the stress relaxation through time: weeks (T1), months (T2) and years (T3) after extraction. The time evolution of the effective core discontinuities points out rock intervals that are variably broken and core segments that remain intact. The Drying Alcohol Discontinuities (DAD) methodology reveals potential discontinuities within apparently intact core segments. By using this technique, a 4-class index is established as a proxy for fissility degree. When integrated with geological, petrophysical and geomechanical data, this index enables characterizing the main mechanisms controlling rock fissility that express through discontinuities promoting the loss of competence of a rock. Consequently, this mechanical property is considered to influence the efficiency of hydraulic fracture in shale reservoir completion.

Keywords: Fissility, Vaca Muerta Formation, Discontinuity, Heterogeneity, Neuquén Basin, Argentina.

RESUMEN. Relación entre fisilidad, composición, fábrica de la roca y propiedades de reservorio en la Formación Vaca Muerta (Cuenca Neuquina, Argentina): del afloramiento al subsuelo. La fisilidad es la capacidad de algunas rocas de partirse a lo largo de superficies suaves paralelas a la estratificación. Es una propiedad observada principalmente en rocas de grano fino, particularmente en afloramiento, donde las mismas se encuentran sujetas al intemperismo. La mayoría de los autores asocian la fisilidad con la abundancia de minerales arcillosos y su orientación paralela a la estratificación. La fábrica horizontal puede ser generada por condiciones depositacionales tales como la composición del sedimento, el contenido de carbono orgánico total (COT) y mecanismo de depositación, dando lugar a una fisilidad primaria. Alternativamente, el alineamiento de minerales laminares puede relacionarse a la historia de soterramiento, por procesos tales como la compactación mecánica o el crecimiento de minerales secundarios, resultando en una fisilidad secundaria. El presente estudio tiene por objeto identificar los principales controles en el desarrollo de la fisilidad a una escala micro- y macroscópica en la Formación Vaca Muerta, expuesta en el área del Cerro Mulichinco y en una corona de 121 m de longitud extraída de un pozo ubicado en la Cuenca Neuquina. En superficie la fisilidad se asocia a facies de grano fino con bajo contenido de carbonato de calcio, revelando un fuerte control litológico. Los valores de COT muestran una correlación positiva entre la riqueza de materia orgánica y la intensidad de la fisilidad. Analizando los ciclos transgresivo-regresivos, se observa que la fisilidad es máxima cerca de las superficies de máxima inundación. Basadas en sus características mecánicas, las interfaces naturales encontradas en la corona se clasifican en interfaces de primer y segundo orden, siendo la fisilidad integrante de esta última clase. Parte de estas interfaces naturales evolucionan de discontinuidades potenciales (parcialmente abiertas) a efectivas (totalmente abiertas), en respuesta a cambios en las condiciones de estrés durante la extracción de la corona y por descompresión a lo largo del tiempo: semanas (T1), meses (T2) y años (T3) luego de su extracción. La evolución de la integridad física de la corona a lo largo del tiempo permite reconocer intervalos de roca que tienden a romperse de manera variable y otros segmentos que permanecen intactos y analizar la evolución de las discontinuidades efectivas. La metodología de Discontinuidades al Secado del Alcohol (DAD, por sus iniciales en inglés) permite revelar las discontinuidades potenciales dentro de los segmentos aparentemente intactos de roca, dando origen a un índice de 4 clases que funciona como un proxy del grado de fisilidad de la roca. Estos resultados se integran con datos geológicos, petrofísicos y geomecánicos a fin de caracterizar los mecanismos que controlan la fisilidad. La fisilidad se expresa como discontinuidades promoviendo la pérdida de integridad de la roca. En consecuencia, esta propiedad mecánica debe influir en la eficiencia del fracturamiento hidráulico de un reservorio no convencional de tipo *shale*.

Palabras clave: Fisilidad, Formación Vaca Muerta, Discontinuidad, Heterogeneidad, Cuenca Neuquina, Argentina.

1. Introduction

Over the last decade, the prolific organic-rich mudstone of the Vaca Muerta Formation has become the main source of unconventional hydrocarbon production in Argentina. It represents the first unconventional self-sourced reservoir that produces "shale gas" and "shale oil" with satisfactory commercial results outside North America (Minisini *et al.*, 2020). The reservoir consists of fine-grained siliciclastic and carbonate rich marine deposits commonly characterized by milimeter-to-centimeter thick laminations. This latter is expressed as an evident bed parallel anisotropy in subsurface and could constitute fissility planes at outcrops. Fissility is the ability of fine-grained rocks to split into slightly uneven flakes, thin chips and wedge-like fragments approximately parallel to the bedding (Lewis, 1924; Ingram, 1953; Pettijohn, 1975, Bates and Jackson, 1987; Sintubin, 1994; Potter *et al.*, 2005). Lewis (1924) referred to this property as a structural characteristic and Ingram (1953) stated that it is more conspicuous on weathered surfaces.

The primary cause of fissility has been attributed to a variety of factors and its origin is still in debate.

Fissility has been largely described at different scales in numerous mudstone outcrops. Some authors proposed that this rock anisotropy derives from mineralogical variation and textural complexity (O'Brien and Slatt, 1990; Slatt, 2011; Ilgen *et al.*, 2017), associated with the diverse sedimentary and diagenetic processes involved in their genesis such as the depositional mechanisms, composition and amount of sedimentary input, redox condition, among many others (Bennett *et al.*, 1991; Potter *et al.*, 2005; Rezaee *et al.*, 2015). Nevertheless, studies analyzing this property in subsurface and their link with the petrophysical properties and the geomechanical behavior of mudstones are scarce.

The stratigraphy of the Vaca Muerta Formation is mainly conformed by mudstones (>85%). The remaining rocks, such as carbonate concretions and tuffs, characterized by a strong rheological contrast with the surrounding mudrock are considered as first order heterogeneities (1 to 6 in Fig. 1). Second order
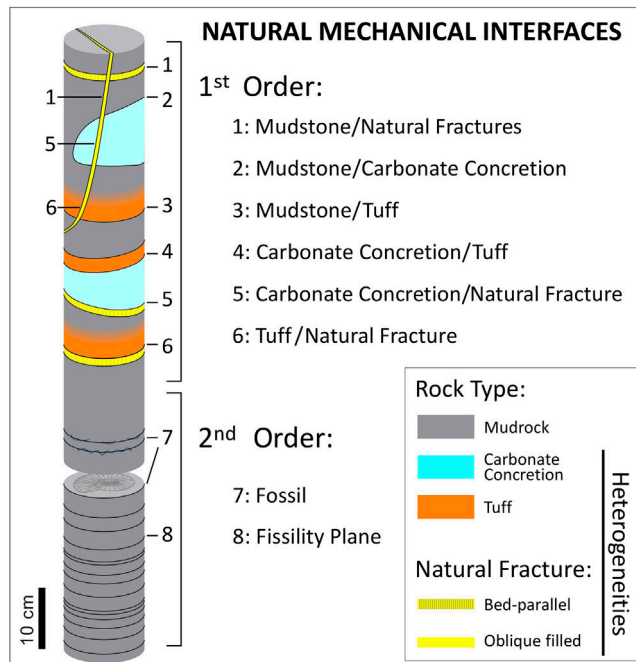
FIG. 1. Classification and nomenclature of the natural mechanical interfaces (black lines) described along the core of well A. All rock volumes/intervals other than mudstones are considered heterogeneities, from meter to millimeter scales. This also includes filled natural fractures: mainly those bed-parallel fractures (BPF or "beefs") and other such as tectonically related oblique fractures. All boundaries between two rock bodies with contrasting mechanical properties (first-order) and all planes that act as mechanical interfaces by themselves (second-order) are considered as natural mechanical interfaces.

mechanical interfaces correspond to the interface itself that generates a local mechanical contrast within a rock presenting the same mechanical properties such as compacted fossils (or their imprint) and fissility planes (7 and 8, respectively in Fig.1). Both heterogeneities and interfaces manifest along a wide range of scales, from outcrop observations, cores, laboratory tests, as far as to the scale of nanometers (Ilgen *et al.*, 2017). These natural interfaces may evolve as an effective discontinuity that splits the rock, or a potential discontinuity within a rock that has not been entirely broken yet. Artificial discontinuities, such as cuts and induced fractures developed during core extraction and preservation are removed from this analysis.

Discontinuity and heterogeneity studies in the Vaca Muerta Formation at different scales have been published by Sagasti *et al.* (2014), Stinco and Barredo (2014), Ortiz *et al.* (2016), González Tomassini *et al.* (2017), Boitnott *et al.* (2018), Casala *et al.* (2019). However, few studies address the role of the fissility planes in mudstones, the main rock type of

Vaca Muerta Formation. King (2010), Walton and McLennan (2013) among others, report that several production anomalies in self-sourced reservoirs are associated with discontinuities and natural fractures, suggesting that these features influence the efficiency of hydraulic fracturing. Vernik and Milovac (2011) propose that bedding-subparallel microcracks may develop in subsurface in overpressured shales. The presence of fissility planes may generate a mechanical decoupling between adjacent blocks, affecting fracture propagation and dissipating additional energy or, conversely, fissility planes may enhance the volume of connected pores by the fracturing process.

This work aims to identify and characterize the main fissility-development controlling factors in the Vaca Muerta Formation mudstones. A synthesis of the current knowledge on fissility in mudrocks, together with the anisotropic mechanical properties, is presented. In the literature, there is a common agreement that fissility in fine-grained rocks only becomes apparent at surface outcrops and is not always evident in fresh core samples (*e.g.*, Lundegard

and Samuels, 1980). Depending on the *in-situ* local state of stress, the rate of core recovery may induce horizontal fractures (Xing *et al.*, 2020). This process defined as core disking (Jaeger and Cook, 1963) occurs in places where mechanical flaws are present. The fissility appears to be time-dependent, arising as a response to weathering (Ingram, 1953; Lundegard and Samuels, 1980; Hurst, 1987). Dewhurst *et al.* (2011) showed that recovery of shale cores from depth causes microfracturing and gaseous exsolution from pore fluids that enhance the anisotropy in the shale fabric. For this reason, the study of well-developed fissility in outcrops exposures, where this property develops clearly, is fundamental. Nevertheless, as the main objective is to understand how fissility affects Vaca Muerta Formation mudstones as an unconventional shale oil and gas play, the focus of this work is the study of this property on core samples. We propose a new methodology to establish a fissility index in relationship to well log and micro resistivity image information. The relationship between fissility and geomechanic rock properties highlights their influence in rock anisotropy.

2. State of the art on mudrock fissility

There are two main contrasting ideas to explain the development of fissility in fine-grained rocks. Most authors (*e.g.,* Ingram, 1953; Gipson, 1965; O'Brien, 1970; O'Brien and Slatt, 1990) argue that fissility is the result of parallel arrangement of platy mineral grains. In contrast, other studies (Pirsson, 1920; Spears, 1976; Curtis *et al.*, 1980) indicate that in some mudstones, particles' parallel orientation is overestimated, whereas lamination and/or stratification are key in fissility development.

Numerous factors can be involved in fissility development (Table 1). These are separated into (**i**) those processes or conditions governing at the moment of sediment deposition, linked with the sedimentary environment, such as the depositional mechanisms and sediment composition, and (**ii**) those developed after mud deposition, such as bioturbation, and during diagenesis such as mechanical compaction, mineral alteration and secondary minerals growth. According to Lewis (1924) in the first case, the fissility would be primary (associated

TABLE 1. CLASSIFICATION OF THE DIFFERENT CONTROLLING FACTORS PROPOSED FOR FISSILITY DEVELOPMENT IN THE LITERATURE.

Fissility type	Controlling factors for fissility development		Influence	Authors
Primary fissility	Depositional mechanism	Floculation		Geikie (1903); Mohr (1932); Kerr (1937); Keller (1946); Krumbein (1947); O'Brien (1970)
		Individual particle settling		
	Sediment composition	Equidimensional minerals		Lewis (1924); Peterson (1944); Grim and Cuthbert (1945); Ailing (1945); Keller (1946); Campbell (1946); Ingram (1953); Hurst (1987); Day-Stirrat *et al.* (2010); Fawad *et al.* (2010); Day-Stirrat *et al.* (2011); Cripps and Czerewko (2017)
		Platy minerals		
	Lamination			Pirsson (1920); Spears (1976); Curtis *et al.* (1980)
	Weak currents	Disorientation		Lewis (1924); Weller (1930); Keller (1946)
		Orientation		
	Bioturbation			Byers (1974); Potter *et al.* (2005)
Secondary fissility	Mechanical compaction			Grabau (1913); Lewis (1924); Pettijohn (1949); O'Brien (1970); O'Brien and Saltt (1990); Lash and Blood (2004); Fawad *et al.* (2010); Crispps and Czerewko (2017)
	Secondary mineral growth	Pervasive mineral growth in random directions		Lewis (1924); Keller (1946); Twenhofel (1939); Payne (1942); Ingram (1953); Pettijohn (1949); Ho *et al.* (1999); Carpentier et al. (2003); Day-Stirrat *et al.* (2010)
		Illite-smectite transformation		

Primary fissility includes all the conditions and processes involved at the sediment deposition time, while secondary fissility is governed by the processes occurring after sedimentation.

with depositional factors), whereas in the second case, the fissility would be secondary (associated with post-depositional processes).

2.1. Primary fissility

Several studies (White, 1961; Van Olphen, 1963; O'Brien, 1970, Table 1) suggest that fissility is favored by the settling of individual platy minerals, parallel to the bedding, while flocculation generates random orientation of clay with poor or no fissility development. The main parameters that promote flocculation, are the type of salt and its concentration (White, 1961), clay content (Rosenqvist, 1966; O'Brien, 1970), absence of organic matter (Van Olphen, 1963; O'Brien, 1970), iron oxides (Peterson, 1944; Ingram, 1953) and stream load (White, 1961).

Grain size and mineral composition affect the development of fissility. In general, the silt content is directly related to the random arrangement of clay minerals (Ho *et al.*, 1999; Olarte and Ruge, 2020). Day-Stirrat *et al.* (2010) showed that illite-smectite bedding-parallel orientation is inversely proportional to the whole-rock quartz content. Experimentally compressed clay-silt mixtures (Fawad *et al.*, 2010) show that (**i**) clay mineral alignment increases with the amount of clay and the effective stress and (**ii**) the alignment of the Illite-smectite fabric is systematically higher than that of kaolinite. Several authors state that organic matter promotes the generation of a parallel clay particles arrangement (Ingram, 1953; Odom, 1967; Hurst, 1987; Cripps and Czerewko, 2017).

In some fine-grained rocks the mineral segregation into thin laminae appears to be the main factor that controls fissility development (Spears, 1976; Curtis *et al.*, 1980). However, the depositional and diagenetic conditions necessary to form and preserve laminations (*e.g.*, absence of bioturbation or pervasive equidimensional secondary minerals growth), enhance the generation of a horizontal-oriented clay fabric parallel to the bedding (Pettijohn, 1975). The preservation of the lamination implies the lack of bioturbation and/or physical reworking (Spears, 1976), suggesting an indirect relationship between lamination and well-oriented fabrics.

Some authors propose that weak currents modify the clay fabric while the sediments are still in contact with the water (O'Brien and Slatt, 1990). Weller (1930) proposes that the random orientation of clay minerals is generated by the stirring wave action. Keller (1946) and O'Brien and Slatt (1990) also suggest that weak currents could reorient platy minerals and promote well-oriented fabric.

2.2. Secondary fissility

Byers (1974) addresses the relationship between the absence of bioturbation and rock fissility, suggesting an early origin dependent on the first stages of mud deposition. In agreement, Sintubin (1994) suggests that stable clay fabrics develop in the early stages of diagenesis, remaining unchanged during the subsequent burial history. Potter *et al.* (2005) established relationships between dissolved oxygen, benthic organisms, sedimentary structures, color, organic matter and pyrite content. Pyrite, commonly present in mudrocks, is formed by the interaction between reactive iron and H_2S after bacterial sulfate reduction in anoxic water column or in sediment pore waters (Berner and Raiswell, 1983). When the redox front is above the water-sediment interface, the resulting mudstone is a well-laminated, dark in color, organic matter rich, commonly with pyrite and scarce bioturbation. On the contrary, when the redox front is below the water-sediment interface, the bioturbation caused by benthic fauna promotes the generation of lighter colored mudstones, with low organic matter content in which the original fabric of the rock has been destroyed.

Mechanical rearrangement during early stages of compaction is one of the main controls on fine-grained fabrics (cf. O'Brien, 1970; Lash and Blood, 2004; Fawad *et al.*, 2010; Cripps and Czerewko, 2017). This process flattens soft particles promoting the collapse and dewatering of floccules, thus producing a rotation and reorientation of the laminar constituents parallel to the bedding.

Growth of secondary phyllosilicates under load have been proposed to explain fissility (Lewis, 1924; Twenhofel, 1936, 1939; Payne, 1942; Pettijohn, 1975). Secondary minerals tend to grow in the direction of minimum stress, commonly parallel to bedding. The smectite-illite transformation, that develops at a narrow range of temperatures, may increase the fabric intensity by a reorientation of phyllosilicates (Ho *et al.*, 1999; Charpentier *et al.*, 2003; Day-Stirrat *et al.*, 2010). However, other diagenetic minerals grow in random directions generating massive rocks, typically carbonates or clay minerals growing in clay gels (Keller, 1946; Ingram, 1953).

3. Geological setting

3.1. Neuquén Basin

The Neuquén Basin (Fig. 2A) extends over an area of approximately 120,000 km^2 in west-central Argentina (Yrigoyen, 1991) and presents a characteristic triangular shape (Legarreta and Gulisano, 1989; Howell *et al.*, 2005; Ramos *et al.*, 2020). The sedimentary sequence is ~7,000 m thick, comprising continental and marine rocks of Late Triassic to Paleogene age.

The origin of the Neuquén Basin is associated with the evolution of the western margin of Gondwana during Late Paleozoic to Early Mesozoic (Uliana and Biddle, 1988; Uliana and Legarreta, 1993; Mpodozis and Kay, 1990; Vergani *et al.*, 1995; Mosquera *et al.*, 2011). Its evolution can be divided into three stages (Fig. 3). The first one corresponds to a Late Triassic-Early Jurassic rifting, in which a series of narrow isolated depocenters developed and were infilled mainly with continental volcanic red-bed facies (Fig. 3A; Manceda and Figueroa, 1993; Vergani *et al.*, 1995; Giambiagi *et al.*, 2008). The rifting stage
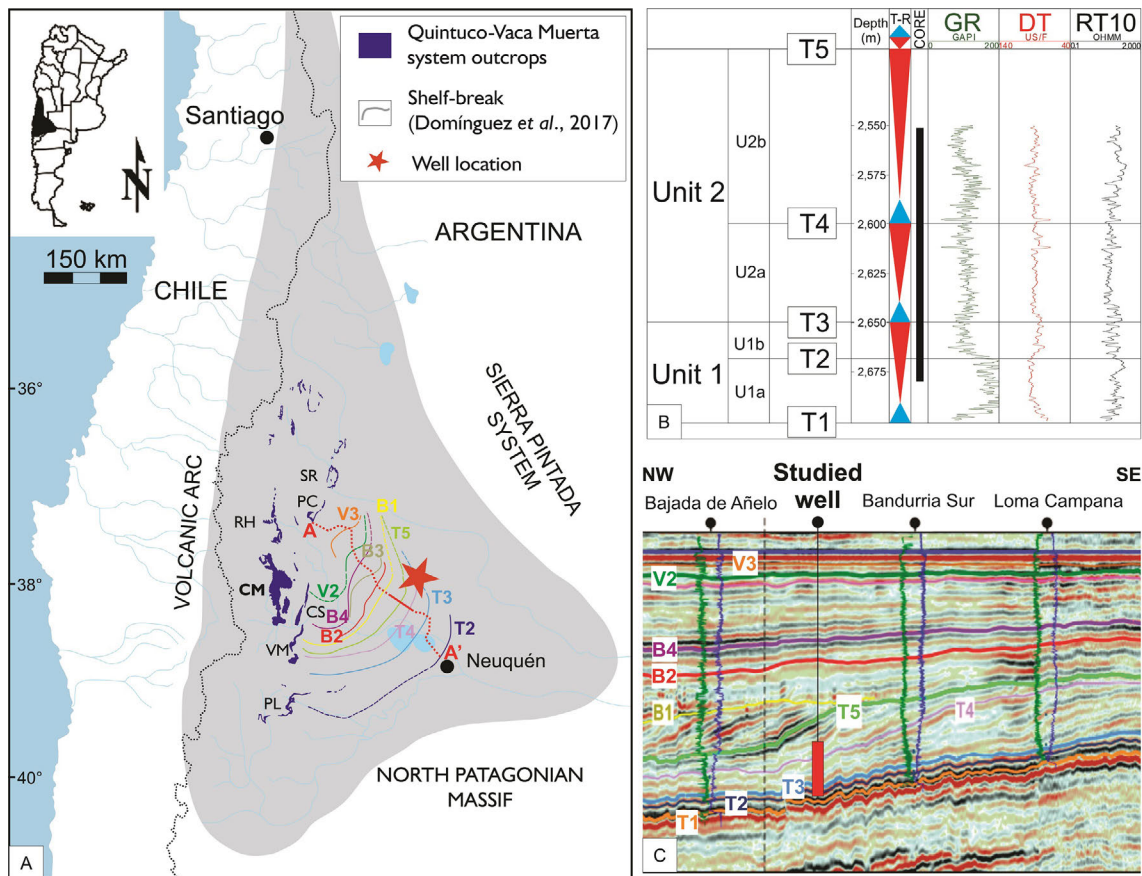

FIG. 2. **A.** Location of the Neuquén Basin (Argentina), well A (red star) and Vaca Muerta Formation outcrops (**SR:** Sierra de Reyes; **PC:** Puerta Curaco; **RH:** Rahueco; **CM:** Cerro Mulichinco; **CS:** Cordón del Salado; **VM:** Sierra de la Vaca Muerta; **PL:** Picún Leufú). Colored lines represent the shelf-breaks of the Vaca Muerta-Quintuco system. Modified from Domínguez *et al.* (2017), using the main seismic horizon nomenclature according to Desjardins *et al.* (2016). **A-A':** northwest seismic section analyzed by Domínguez *et al.*, 2016. **B.** Subdivision of Vaca Muerta Formation: T1 to T5 are seismostratigraphic l horizons regionally defined (Desjardins *et al.,* 2016) correlated to well A, subdividing the shale play into 2 principal units (**Unit 1:** Lower Vaca Muerta; **Unit 2:** Upper Vaca Muerta) and 4 subunits (U1a, U1b, U2a and U2b) based on well logs response. Blue and red triangles represent the transgressive-regressive cycles. Black vertical bar: cored interval. **GR:** gamma ray log; **DT:** sonic log; **RT10:** resistivity log. **C.** Seismic section A-A' displaying the location of the surfaces defined by Desjardins *et al.* (2016) and the extension of the studied core (in red). Modified from Sattler *et al.* (2016).
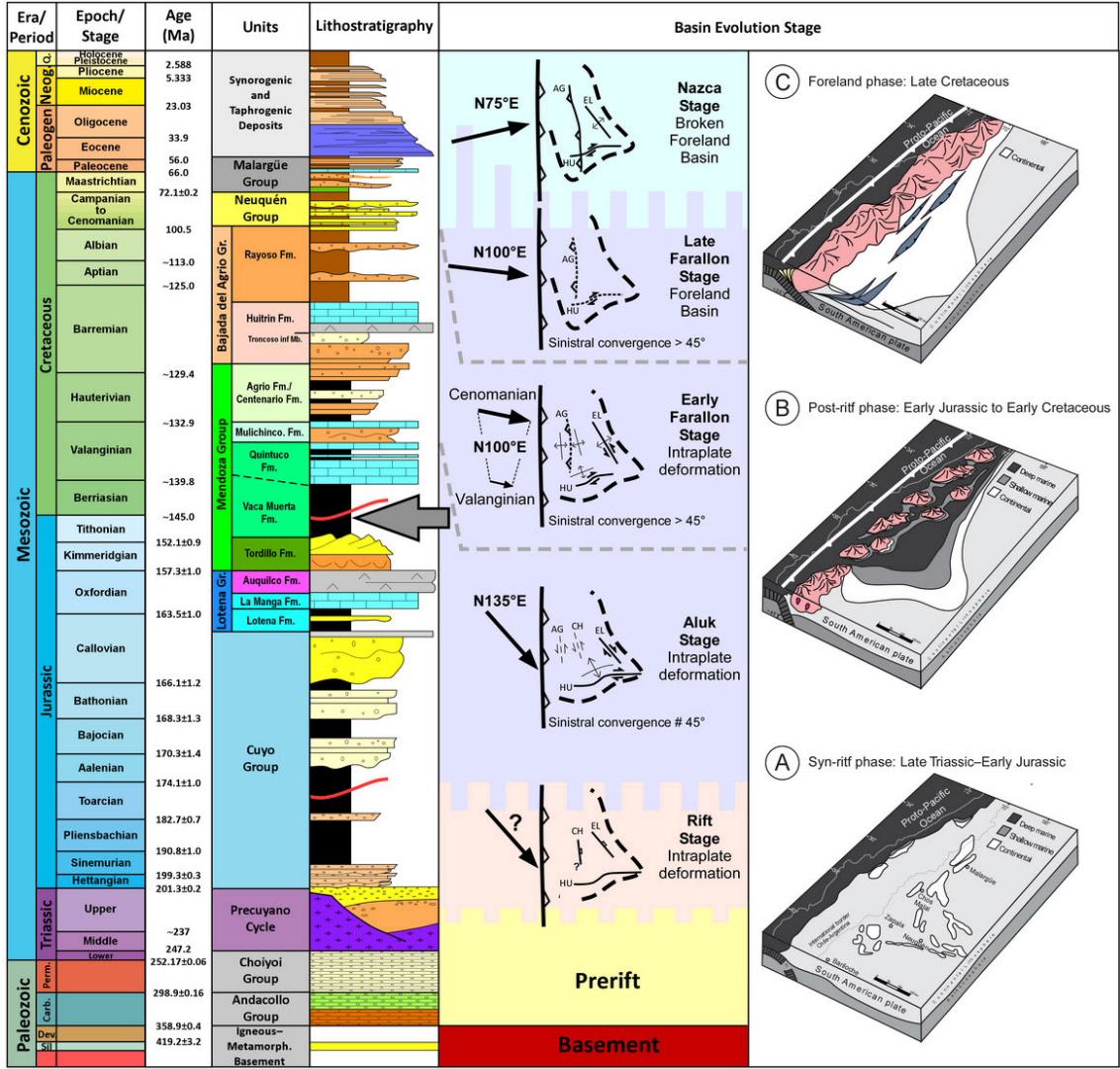
FIG. 3. General stratigraphic chart showing main stages of Neuquén Basin evolution (A-C) and the studied interval (gray arrow). Modified from Howell *et al.* (2005) and Marchal *et al.* (2020).

was followed by a widespread thermal subsidence accompanied by the development of an Early Jurassic to Early Cretaceous back-arc basin (Fig. 3B; Vergani *et al.*, 1995). In this period the Neuquén embayment consisted in a partially closed basin, limited to the west by a low-topography volcanic arc, connected to the Paleopacific Ocean only through few narrow marine passages (Spalletti *et al.*, 2000; Macdonald *et al.*, 2003; Howell *et al.*, 2005). The sedimentary deposits resulted from the combination of eustatic oscillations, subsidence rate variations and tectonic movements that allowed the accumulation of thick sedimentary deposits, including evaporite sequences and non-marine clastic sediments, frequently under fast marine flooding events (Legarreta and Uliana, 1991; Legarreta, 2002; Legarreta and Villar, 2015). From Late Cretaceous to Cenozoic, the tectonic regime became compressive, leading to the uplift of the foreland thrust belt, although extensional events had been recorded (Fig. 3C; Ramos and Folguera, 2005; Ramos, 2010; Legarreta and Uliana, 1991; Ramos, 1999). During this last period, over 2,000 m of continental syn-orogenic sediments were deposited due to flexural subsidence towards the east of the tectonic front (Legarreta and Uliana, 1991; Ramos, 1999).

3.2. Vaca Muerta Formation

The Vaca Muerta Formation (Weaver, 1931) is part of the sedimentary infill of the Neuquén basin. It corresponds to the most distal facies of Lower Mendoza Group Mesosequence (Legarreta and Gulisano, 1989: Fig. 3), developed by a rapid and widespread marine transgression from the Paleopacific Ocean during early Titonian-early Valanginian (Mutti *et al.*, 1994). It is mainly composed of dark bituminous and calcareous mudstones and limestones (Legarreta and Uliana, 1991, 1996; Kietzmann *et al.*, 2008, 2014) deposited in a mixed siliciclastic-carbonate ramp environment favorable for the accumulation of organic matter type I/II (Legarreta and Villar, 2012). The Vaca Muerta Formation lies over the Tordillo Formation or the Lotena Group (towards the north of the basin) or even directly on top of the Cuyo Group towards the south of the basin (Garcia *et al.*, 2013). The Vaca Muerta Formation grades eastward into shoreface deposits (Quintuco Formation) and sabkha deposits (Loma Montosa Formation, Mitchum and Uliana, 1985; Gulisano *et al.*, 1984; Carozzi *et al.*, 1993; Krim *et al.*, 2017). The top of the Vaca Muerta Formation is diachronous and becomes younger towards the northwest of the basin (Legarreta and Gulisano, 1989; Lazzari *et al.*, 2015; Krim *et al.*, 2017).

The studied outcrop is at Cerro Mulichinco area, ~20 km northeast of Loncopué, about 270 km NW of Neuquén city (CM in Fig. 2A). This area, belonging to the Loncopué Through, corresponds to the thickest stratigraphy (~1,100 m) of the Vaca Muerta Formation, where the base and roof contacts with the Tordillo and Quintuco formations are respectively exposed (Fig. 4). In this locality the Vaca Muerta Formation is composed of dark laminated and massive fossiliferous claystones and siltstones with calcareous mudstone intercalations. Bedding parallel fractures filled with fibrous calcite, commonly referred to as 'beefs' or 'bedding parallel fractures (BPF)', are up to 5 cm thick (Rodrigues *et al.*, 2009; Ukar *et al.,* 2017, 2020). Layers with carbonate concretions are conspicuous, displaying spherical or ellipsoidal forms that vary from 5 to 70 cm length along their major axis (exceptionally reaching 1 m, Otharán *et al.*, 2020; Rodríguez Blanco *et al.,* 2022). Friable volcaniclastic levels are frequent towards the bottom of the Formation, commonly orange in color due to pervasive ferric oxides and clay content, frequently referred to as bentonites (Lejay *et al.*, 2017; Minisini, 2017).

The studied well A is located within the morphostructural region of the embayment of the Neuquén Basin (Fig. 2). The Vaca Muerta Formation in this region is in the oil window and is composed of fine-grained sediments (mainly calcareous mudstone) deposited in a basin-external ramp environment. The studied stratigraphic interval includes rocks from the middle and lower part of unit 2 (between T5 and T3 seismostratigraphic horizons, according to Desjardins *et al*., 2016; Fig. 2B) and the upper part of unit 1 (between T3 and T1 in Fig. 2B) defined by Sattler *et al*. (2016). Unit 2 includes two intervals: U2b, known informally in the industry as 'Orgánico superior' one of the main targets in the basin center, and U2b, named as 'Orgánico inferior' between T4 and T3 surfaces. Unit 1 is subdivided into U1b, informally denominated as 'Parrilla' between T3 and T2, and U1a known as the 'Cocina', an important target included between T2 and T1 (see Fig. 2B).

4. Materials and methods

4.1. Outcrop

In a first field campaign, a general sedimentary section of the Vaca Muerta Formation was elaborated at the locality of Arroyo Mulichinco (east side of the Cerro Mulichinco area, Zavala *et al.*, 2015; Otharán *et al.*, 2020) (Fig. 4). This section was studied sistematically with 1 Kg rock samples every meter obtaining more than 350 specimens. A subsequent field campaign focussed on mudstones fissility and concentrated on the lower 500 m of the column. The mudstones were classified visually into five fissility classes (following O'Brien, 1970) depending on how they fracture when broken. The first one represents a well-developed fissile mudstone that splits into very thin slabs with smooth surfaces parallel to the bedding whereas the fifth class corresponds to massive rocks. Mudstones with moderate to poor fissility split into thicker slabs with undulatory fracture surfaces.

The fissility degree from each sample was quantified by measuring the fragments width with a digital caliper. All samples were analyzed by Total Organic Carbon (TOC) content and a petrographic description was carried out, for the different fissility classes, to characterize their composition and fabric.
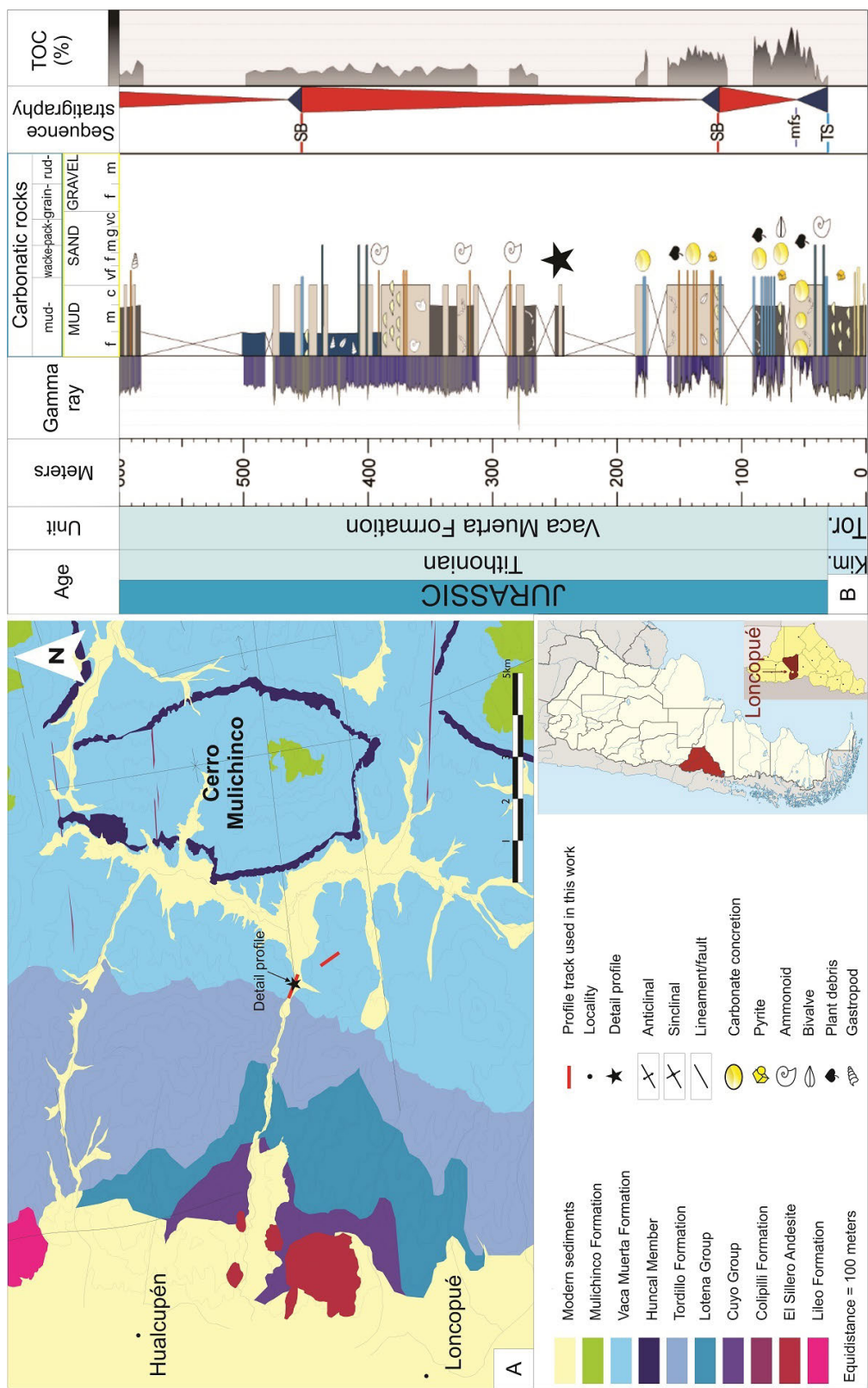
FIG. 4. Cerro Mulichinco outcrop. **A**. Location map of the studied outcrop. Red lines indicate the stratigraphic profiles used in the present study, black star indicates location of detailed profile presented in figure 7 (Arroyo Mulichinco). **B**. General simplified stratigraphic and lithologic log of Cerro Mulichinco outcrop with the transgressive-regressive (T-R) cycles (blue and red triangles) and TOC content, indicating the stratigraphic location of the detailed profile at "Arroyo Mulichinco" (black star) modified from Otharán (2020). Rock classification: Carbonate (Dunham, 1962), Siliciclastic (Pettitjohn, 1975).

In a well-exposed outcrop with contrasted rock fissility intervals, a detailed 6 m long profile was elaborated, measuring the fissility density every 5 cm (Fig. 4). The carbonatic and siliciclastic facies were described considering lithology, sedimentary structures and bedding geometry. A two letter facies code was used: the first one represents lithology and the second one sedimentary structures or fabrics. Sedimentary environments subdivisions follow Burchette and Wright (1992). Sedimentological interpretations and thin section descriptions of samples were used to establish the relationships between sedimentological processes and fissility development.

4.2. Subsurface datasets

The analysis of the subsurface information was performed on a 121 m long core from well A, located at the center of the Neuquén Basin (Fig. 2).

The study describes all effective and potential discontinuities. Effective discontinuities are those that split the rock into different pieces, while the potential ones do not separate the core into distinct blocks (Fig. 1) at the time of the different measurement and description.

Effective discontinuity planes distribution was recorded at three different times (from core extraction to present). The initial state at time T1 corresponds to the effective discontinuity planes expressed after seven weeks of core extraction and transportation. Core state at time T2 comprises the additional effective discontinuity planes developed after the slabbing and description of the core, approximately fourteen months after core extraction. Lastly, time T3 corresponds to the distribution of the effective discontinuity planes after five years of core storage. The comparison of effective discontinuity frequency at the three different times allowed the recognition of intervals that tend to break over time and core intervals that remain unbroken.

A new methodology is presented to estimate the potential fissility grade of rock in a core, based on the observation of evaporation on core surfaces sprayed with alcohol. This procedure highlights small discontinuities within the apparently intact rock. The fluid tends to concentrate within the rock discontinuities (many imperceptible to the naked eye), thus during evaporation process they are the last to dry (Fig. 5A). Those discontinuities exhibit a variable frequency along the interval and are considered as potential

fissility planes. To classify the rock intervals as a function of the mean discontinuity spacing, 262 photos were taken and used to elaborate a semi-quantitative frequency scale. All photos were taken with a tripod, at 30 cm from the camera and 15 seconds after the sample was sprayed with alcohol. The pictures were subsequently classified according to the potential discontinuities spacing into 4 classes that define a Drying Alcohol Discontinuities (DAD) index as a proxy for fissility tendency (Fig. 5B). The first class corresponds to the maximum fissility and the fourth class to a massive rock. Thin sections, X-ray diffraction (XRD), calcimetry and total organic carbon (TOC) measurements, together with X-ray fluorescence (FRX) measurements allow the geochemical, mineralogical and fabric characterization of each DAD index class. The DAD index is finally upscaled using a sample rate of 0.1 m for correlation to well logs.

The microresistivity logs are processed in conjunction with the fissility data, in which two parameters were evaluated: (**i**) the lamination density obtained from the customized and controlled automatic dip picking, at a sample rate of 0.1 m, and (**ii**) a mean resistivity obtained from the averaged pads calibrated with the shallow resistivity log that provided a higher resolution porosity log. This curve is calibrated with other porosity logs and subsequently compared with the DAD index.

The study of the fissility property on the electric logs is based on a supervised classification that generates four electrofacies to reproduce the DAD clases along the well. An electrofacies is defined as the set of log responses which characterizes a rock interval and permits it to be distinguished from the others (Doveton, 1994). This methodology consists in providing to the software the input information (in this case the DAD index) in order to build a model where each electrofacies corresponds to a DAD class. By using the Facimage analysis tool from Geolog™ Formation Evaluation software (based on Multi-Resolution Graph-based Clustering: MRGC) numerous combinations of well logs were run to reproduce the DAD index along the cored interval. The best combination obtained from this classification consists of gamma ray and photoelectric absorption factor that represents lithology, shallow resistivity that includes texture information and compressional slowness as a proxy of geomechanical properties.

The relationship between the mechanical behavior of the fissility classes was established by
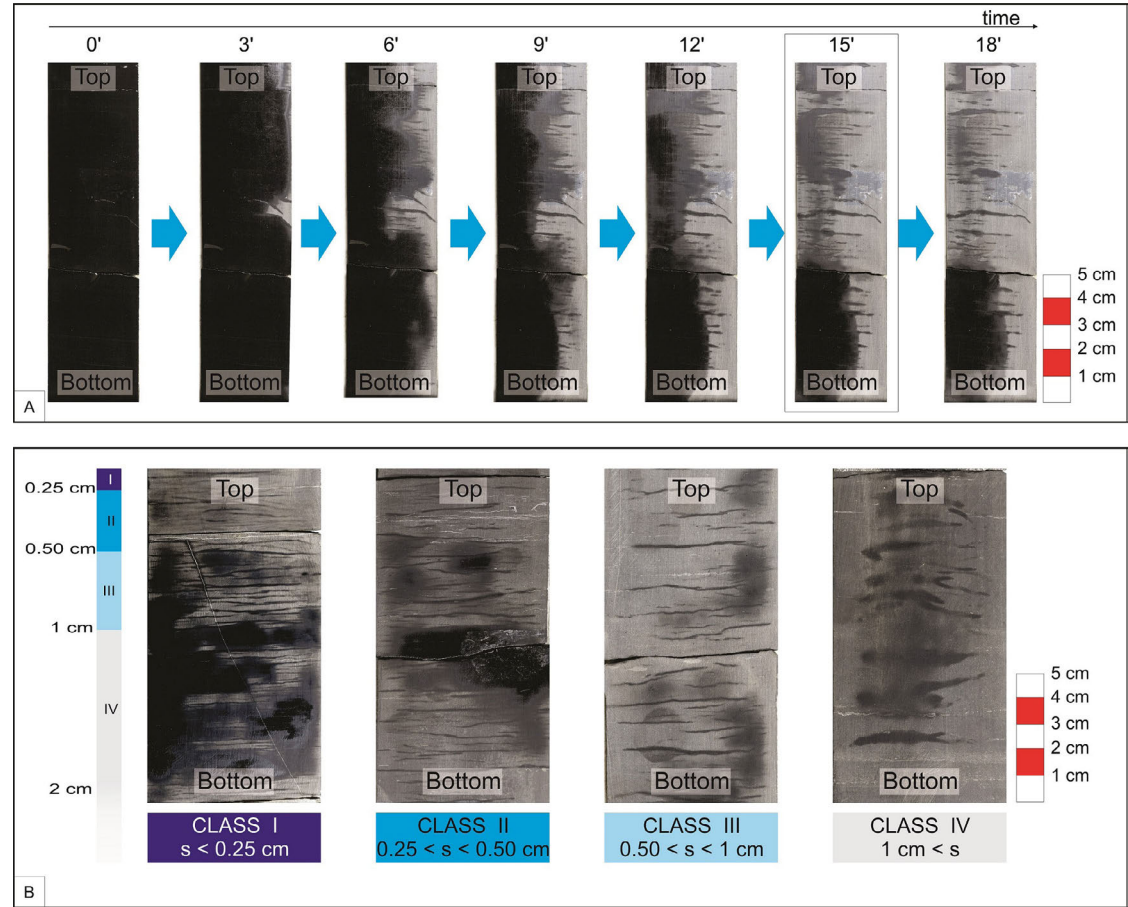
FIG. 5. Drying Alcohol Discontinuities (DAD) method for fissility planes identification in well A core. **A.** Drying sequence on a slabbed and polished core showing several discontinuities along time. Optimum time to estimate the higher density of discontinuities is 15 seconds after spraying. **B.** The 4 DAD classes defined by the spacing (s) between potential discontinuities revealed by the alcohol drying.

correlation with geomechanic laboratory testing. The rock mechanic data includes uniaxial compressive strength (UCS), multistress compressive testing and elastic parameters, as Young modulus, Poisson ratio and static and dynamic shear modulus.

5. Results

5.1. Outcrop study

Following Kietzmann *et al.* (2021), nine lithofacies representing sedimentary processes were grouped into four facies associations, corresponding to subenvironments representing different energy sedimentary conditions (Fig. 6):

- Facies association F1: poorly laminated medium gray mudstones (Mn) with a characteristic nodular texture (Fig. 6A). The beds are tabular with sharp and planar contacts. Occasional orange patches are observed, probably corresponding to ferric oxides and hydroxides.
- Facies association F2: alternation of laminated dark gray mudstones (Ml) and laminated wackestones (Wl), normally under 5 centimeters thick (Fig. 6B). Subordinated centimeter thick tuffs (Tm/l) and laminated calcareous mudstones (Mcl) also occur.
- Facies association F3: dominated by wackestones usually laminated (Wl) and laminated calcareous mudstones (Mcl). Occasionally occur centimetric

	Lithofacies		Facies association			
			F1	F2	F3	F4
Low energy	Laminated mudstone with nodules	Mn	MR			
	Laminated mudstone	Ml		MR		
	Laminated wackestone	Wl		R	MR	
	Laminated calcareous mudstone	Mcl		S	MR	R
High energy	Laminated fine grained sandstone	Sh			S	
	Massive packstones	Pm			R	MR
	HCS packstones	Phcs			R	MR
	Laminated packstone	Pl			MR	R
	Massive or laminated tuff	Tm/l		S	MR	R

FIG 6. Sedimentary facies identified at Arroyo Mulichinco profile. **A.** Facies association F1: poorly laminated medium gray mudstones (Mn) with nodular texture. **B.** Facies association F2: alternation of laminated dark gray mudstones (Ml) and laminated wackestones (Wl) and calcareus mudstone (Mcl). **C.** Facies association F3: wackestones usually laminated (Wl) and laminated calcareous mudstone (Mcl) with occasional laminated packstones (Pl) and hummocky cross-stratified packstones (Phcs) centimetric beds. **D.** Facies association F4: massive packstones (Pm), hummocky cross-stratified packstones (Phcs) and laminated calcareous mudstones (Mcl). E. Synthesis of most representative (MR), representative (R) and subordinate (S) lithofacies for each facies association.

beds of laminated packstones (Pl) and hummocky cross-stratified packstones (Phcs) and scarce fine sand levels with poor horizontal lamination (Sh). The biodiversity observed in these rocks is low, mainly radiolarians, scarce foraminifers and indeterminate fragments of bivalves. Towards the top are ammonoids lying parallel to bedding. Intercalations of orange volcanic levels are common, pervasively altered to clays and ferric oxides that hinders the identification of their original structure, although horizontal lamination can be locally determined. These facies commonly include levels rich in carbonate concretions that vary from 15 to and 30 cm long (Fig. 6C).

• Facies association F4: massive packstones (Pm), hummocky cross-stratification (Phcs, Fig. 6D) and laminated calcareous mudstones (Mrl). This facies association includes the thickest volcanic levels of approximately 15 cm. The beds are tabular, approximately 20 cm thick, with sharp planar bases and tops. The carbonate concretions levels of larger diameter are associated with the packstones lithofacies, displaying up to 50 cm thick beds (Fig. 6B).

Figure 6E synthetizes the different lithofacies present in this section, discriminated between low and high-energy facies. The low energy lithofacies represent sedimentation in fair-weather conditions, dominated by settling of fine-grained suspended material. On the contrary, high-energy lithofacies suggest a deposition dominated by tractive flows, associated with storm events that result in hummocky cross-stratification. Vertical arrangement of these facies allows the recognition of small fluctuations in water depth and environmental energy. These small variations can be assimilated to high frequency transgressive-regressive cycles (Fig. 7) in an outer to mid ramp environment (Kietzmann *et al.*, 2016).

The 4 different facies associations are all interpreted to be deposited in a poorly oxygenated outer ramp below the storm wave base: facies association 1 and 2 are more distal (with facies association 1 slightly deeper than facies association 2) than facies association 3 and 4, which are close to the storm wave base.

The fissility classification of the Cerro Mulichinco rock samples is shown in figure 8, together with a picture illustrating their fabric and their respective petrographic interpretation. In general, massive mudstones without fissility are also massive under the microscope or might have a poorly defined lamination. Their fractures

are usually conchoidal, discontinuous and with a random orientation with respect to the bedding. In contrast, high fissility rocks under microscope show platy particles (minerals, bioclasts, organic matter) oriented parallel to the bedding, frequently showing higher fissility when their components are discretized in layers. Their well-developed fissility planes are straight, smooth and fine-spaced.

The visual classification of the samples displays a good correlation between fissility and the average width of the fragments as well as with their TOC values (Fig. 9). The more fissile the sample, the thinner their fragments and higher their TOC. Almost all the samples with high fissility (classes 1 and 2) have a TOC over 4%, whereas the rest of the classes have a wide range of TOC, except for the massive samples (class 5) that exhibit TOC under 4%.

5.2. Subsurface data

The analyzed core interval includes mainly calcareous and mixed mudstones, occasionally laminated, constituting 75% of the core (Fig. 10). Around 18% of the rocks are siliciclastic mudstones that tend to concentrate towards the bottom of the core. There are minor quantities of carbonate intervals, mostly associated with microbial precipitation or diagenetic processes. Subordinated tuffs represent about 2% of the lithologies.

5.2.1. Core analysis

The study of effective discontinuity planes (EDP) distribution through time (Fig. 10) was performed identifying 4 different types (Fig. 1): (**i**) first-order interfaces occur at lithologic contacts (carbonate concretion and tuffs) with the surrounding mudstone and at bed-parallel fracture borders and (**ii**) second-order interfaces correspond to fossil imprints and fissility planes. Figure 10 displays the evolution of these discontinuities along the core through time (T1, T2 and T3). Most of the mapped discontinuities are fissility planes and their proportion remains almost constant (55 to 60%) through time. The discontinuities associated with lithologic contacts represent 17% at T1, decreasing until 12% at T3. Those discontinuities associated with bed-parallel fractures show a similar trend, decreasing from 14% at T1 to 9% at T3. Discontinuities associated with the presence of fossil imprints show the opposite tendency, increasing from 14% to 20%.
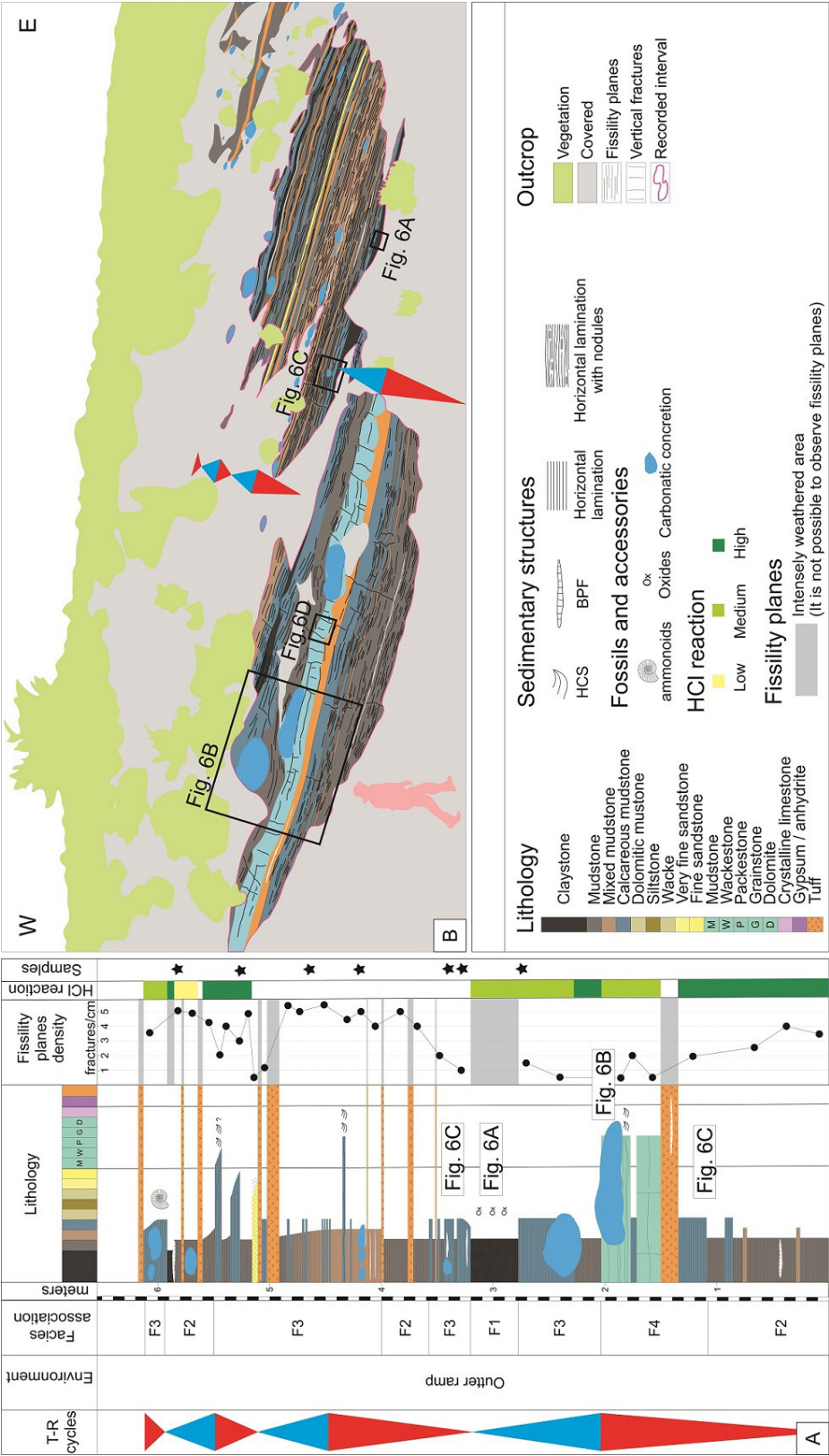
FIG 7. Fissility study at Arroyo Mulichinco outcrop, Cerro Mulichinco area. **A.** Detailed stratigraphic profile showing the sequential interpretation (T-R cycles represented by the blue and red triangles, respectively), facies association, lithology, fissility planes density (count of fissility planes with 5 cm windows), HCl reaction and sample location. **B.** Line drawing of the outcrop and lithologic and sedimentary interpretation. Labels "Fig. 6A-D" indicate the location of the photos presented in figure 6. **HCS:** Hummoky Cross Stratification. BPF: Bed-Parallel Fracture.

Scale	Class	1	2	3	4	5
Outcrop	Fissility	VERY WELL DEVELOPED	WELL DEVELOPED	DEVELOPED	MODERATE-POOR	NONE
	Photography					
	Average fragment width (mm)	3	5	8	15	21
Thin section	Microphotography					
	Lithology	Silicoclastic mudstone	Microbialitic bindstone	Silicoclastic mudstone	Microbialitic bindstone	Bioclastic wackestone
	Interpretation					
	Discontinuity planes	+ Highest density. + 0.05 mm average spacing. + Follow the fabric of the rock. + Often bifurcate or truncate each other.	+ Density higher when the rock is layered. + 1 mm average spacing. + Irregular and follow the material morphology. + Frequently connected by subvertical / oblique fractures. + Principally tape gradually, mostly discontinuous. + Only a few breaks through the whole petrographic section.	+ Few observed, generally located at the interphase between different composition layers. + Spacing variable, ranging from 5 and 20 cm. + Irregular, discontinuous, occasionally bifurcate or become oblique. + Tape gradually into the rock.	+ Scarce. + very irregular and laterally restricted. + Tape gradually into the petrographic section. + Occasionally break through carbonatic skeletal fragments.	+ Not observed.

straight morphology ⟵

smoother surface ⟵

finer spacing between discontinuity planes

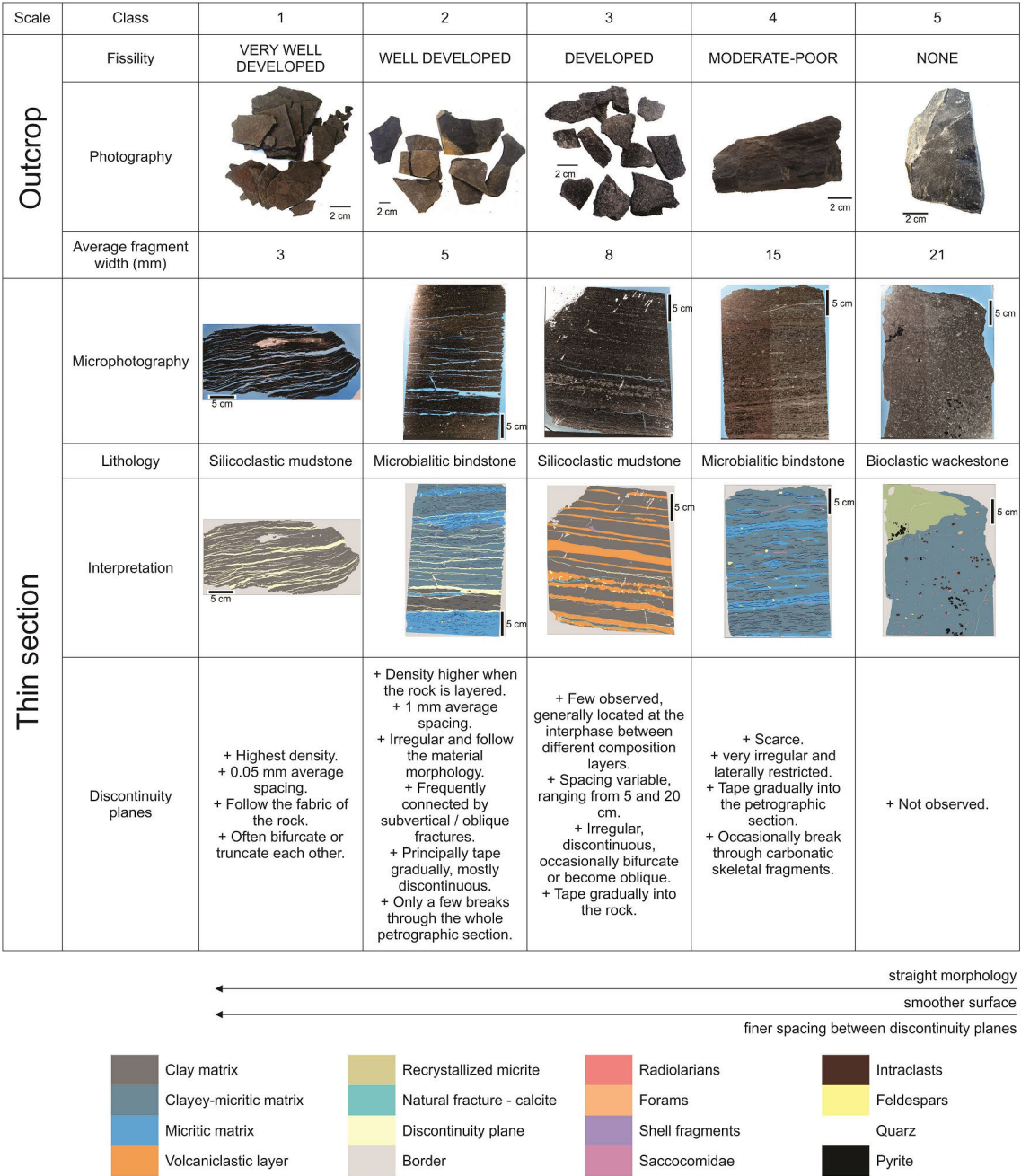|				
▮ Clay matrix	▮ Recrystallized micrite	▮ Radiolarians	▮ Intraclasts	
▮ Clayey-micritic matrix	▮ Natural fracture - calcite	▮ Forams	▮ Feldespars	
▮ Micritic matrix	▮ Discontinuity plane	▮ Shell fragments	▮ Quarz	
▮ Volcaniclastic layer	▮ Border	▮ Saccocomidae	▮ Pyrite	

FIG 8. Visual fissility classification based on O'Brien (1970) displaying the main characteristics for each class at outcrop and microscope scales. Note that the spacing between horizontal discontinuities (interpreted as fissility planes) becomes narrower towards the first class (very well-developed fissility) while the massive samples (class 5, none fissility) lack horizontal discontinuities. The samples corresponding to the very well developed fissility class present discontinuities that often truncate each other.
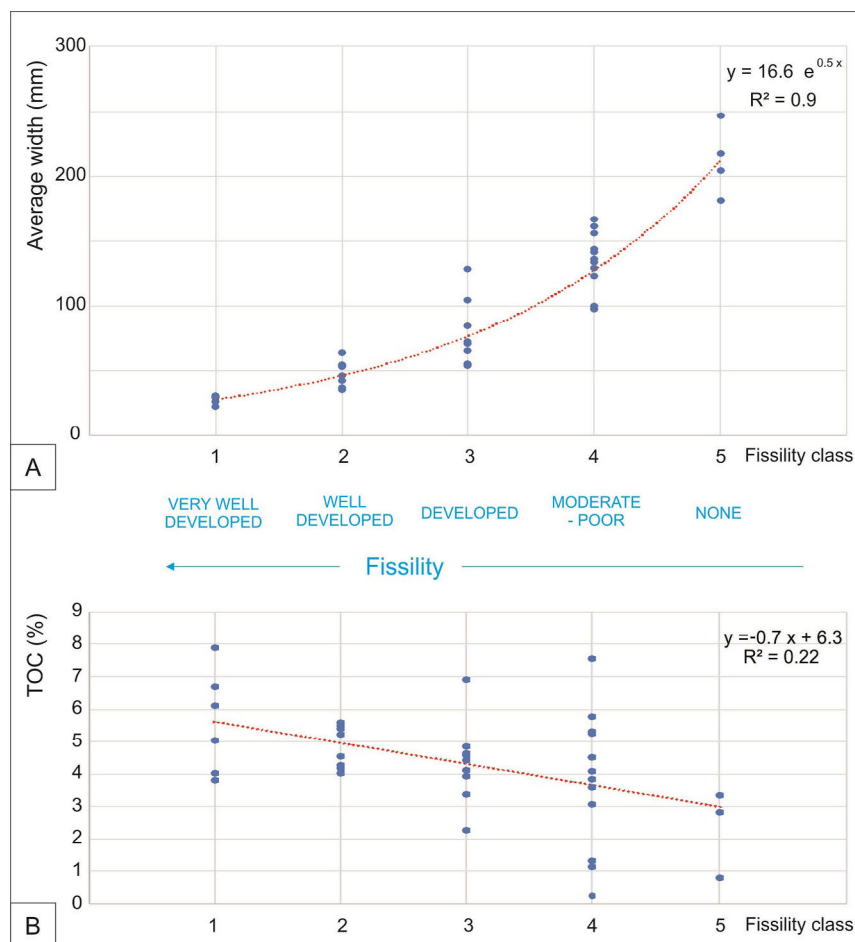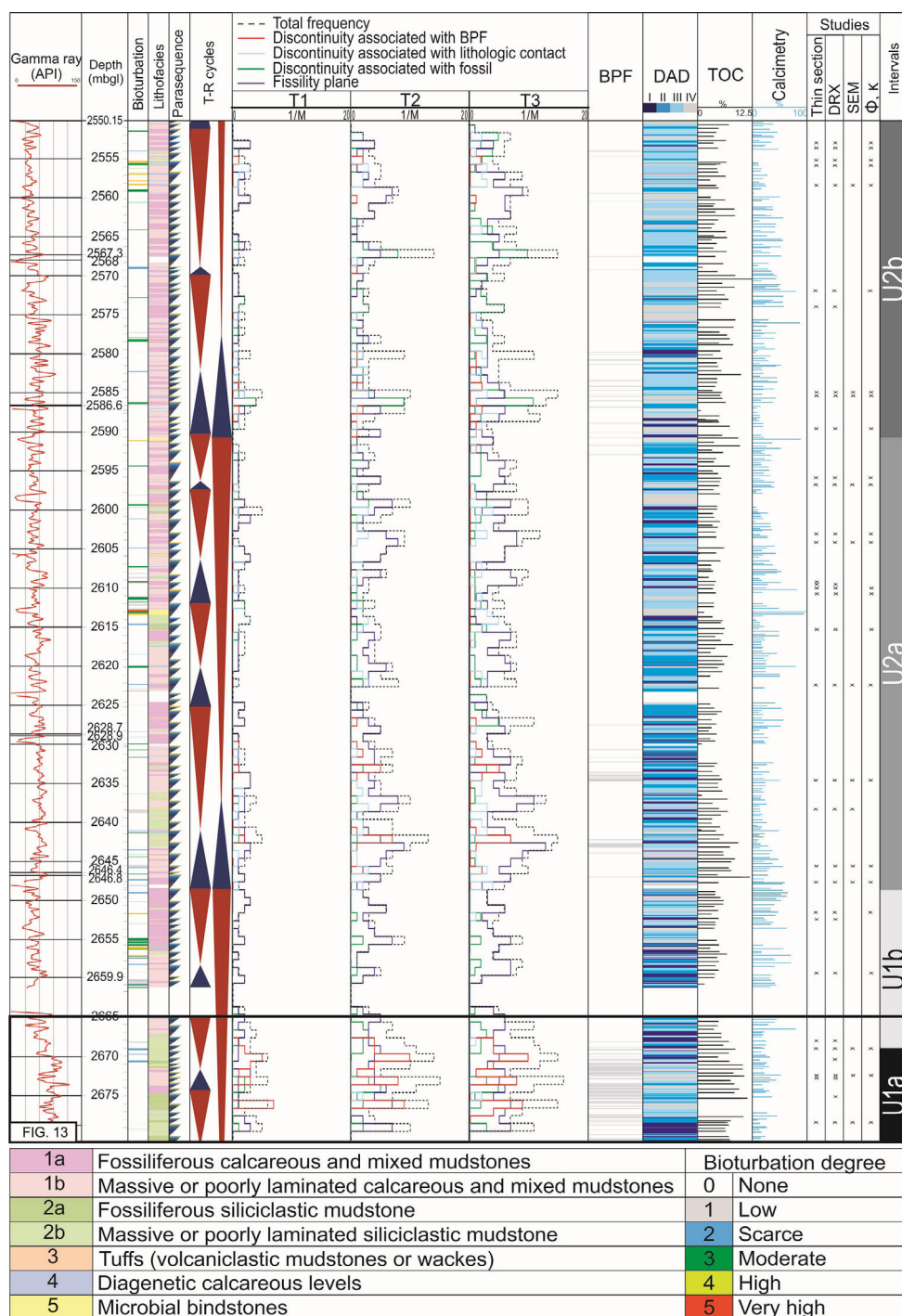
FIG 9. Fissility class characteristics at Arroyo Mulichinco outcrop. **A.** Average fragment width for each fissility class of O'Brien (1970). **B.** TOC content in sedimentary rocks according to fissility class, showing the tendency of high fissility rocks to be organic richer than massive-ones.

The analysis of the density of EDP through time shows that they develop preferentially in high fissility intervals (DAD I or II, Figs. 10 and 11A, T1 to T3). The evolution through time of the different discontinuity types (Fig. 11B) reveals that the greatest increment occurs from T1 to T2, where all types of discontinuities in T2 almost double and triple the amount of EDP in T1 (increment factor of 1.9 to 3.8, Fig. 11B). In general, the rate of generation of EDP at this time is greater for second order discontinuities (fissility planes and discontinuities associated with fossils) than for first order discontinuities (associated with lithologic contacts and BPF). From T2 to T3 the EDP displays a growth of approximately 50% (incremental factor

about 1.5), except for the EDP associated to BPF, with a quantity only about 7% in T3 more than the previous T2. Finally, the ratio of first order to second order EDP diminishes through time (Fig. 11C). In the studied core interval, a strong correlation between the evolution of the natural discontinuity density and the DAD fissility index is observed. The comparison between the 3 frequency curves (Fig. 10) shows that rocks which tend to break with high density correspond mainly to the high fissility classes (DAD I and II), whereas core intervals that remained mostly unbroken correlate with none or low fissility classes (DAD III and IV).

Regarding the DAD index and rock properties, the same relationships are observed in subsurface
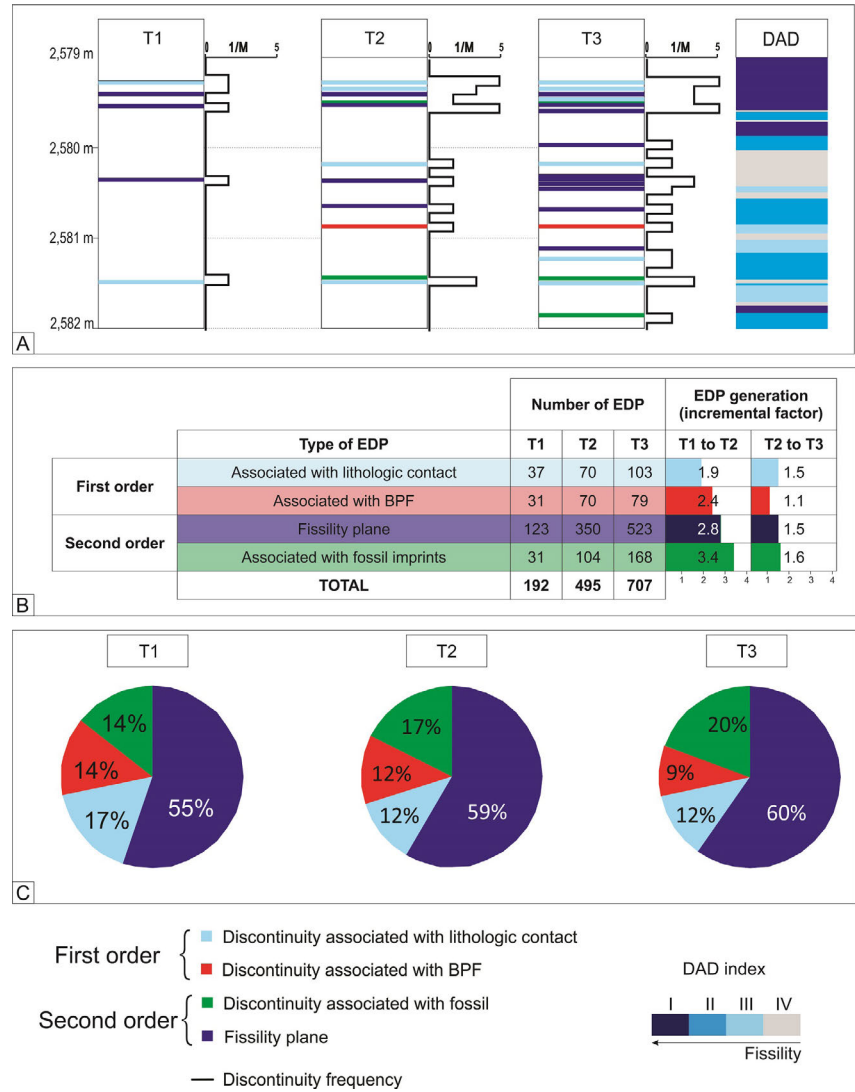
FIG. 10. Relationship between DAD index and well A core information. Transgressive-Regressive (T-R) cycles represented in blue and red triangles, respectively. Discontinuity plane density at three different times: **T1:** 7 weeks after core extraction (entire core); **T2:** 14 months after core extraction (slabbed); **T3:** 5 years since core extraction (slabbed). First order discontinuities: interfaces at lithologic contacts (principally mudstones-tuffs and minor quantities of mudstones-carbonate concretion) and interfaces between bed-parallel fractures (BPF) and their surrounding rocks. Second order discontinuities are associated with fossil imprints and fissility planes. Depth in meters below ground level (mbgl). Lower rectangle indicates the interval included in figure 13. The sequencial interpretation and the bioturbation index are based on Otharán (2020) and Otharán *et al*. (2022).

FIG 11. Evolution of fissility and discontinuity planes through time of the well A core: presence, distribution and clustering of the different discontinuity plane types. **T1:** discontinuity planes after seven weeks of core extraction and transport. **T2:** discontinuity planes after core slabbing and description (fourteen months of core extraction). **T3:** discontinuity planes after core storage for five years. **A.** Example of Effective discontinuity planes (EDP) distribution at a specific depth through time. **B.** Generation of EDP through time and incremental factor between two different time steps. **C.** Proportion of different discontinuity plane types at the three different times.

samples and in outcrop exposure concerning the TOC and carbonate contents (Fig. 10). In general, the rock intervals with higher fissility (DAD I and II) are fossiliferous siliciclastic mudstones and massive to poorly laminated siliciclastic mudstones that are more conspicuous towards the base of the Vaca Muerta Formation (Fig. 10). Some calcareous and mixed mudstones correspond also to high fissility

classes. These rocks display high TOC values (>4%) and low carbonate content (<40%, with an average around 18%).

The rocks that remain massive (DAD III and IV) are mainly calcareous and mixed mudstones, volcaniclastic mudstones, diagenetic calcareous levels and microbial bindstones (Fig. 10). The lithofacies 4 and 5 (Fig. 10) univoquely correspond

to the DAD class IV and display a low TOC average content (3%), with noticeable variance. As expected, carbonate content is higher, especially in DAD class IV rocks, with an average of around 50%.

When present, bed-parallel fractures (BPF or "beefs") show a variable relationship with the fissility index (Fig. 10). Especially towards the upper part of the core the BPF occurrence is mostly associated with high fissility mudstones (DAD classes I or II). Nevertheless, there are some high fissility rocks where no BPF are visible as well as massive rocks (DAD classes III or IV) with high frequency of bed-parallel fractures.

The degree of bioturbation is mapped following Lazar *et al.* (2015) scale, where 0 corresponds to absence of bioturbation and 5 indicates total bioturbation and was extracted from Otharán (2020) and Otharán *et al.* (2022) (Fig. 10). As expected (Byers, 1974; table 1), a strong correlation between the medium to high bioturbated mudrocks (≥3) with the massive intervals is observed (DAD IV; Fig. 12).

From a sequence stratigraphy point of view, the DAD index shows a good correlation with the transgressive-regressive cycles. Regressive intervals frequently start with rocks corresponding to DAD classes I or II, becoming more massive (DAD III or IV) towards its end. The opposite occurs at transgressive sequences, where the rocks begin as low or none fissile, becoming highly fissile towards the end of the hemicycle (Fig. 13A). A relationship between the DAD index and the sequences is clearly established, even at the parasequence scale (Fig. 13B). Shallowing upward parasequences commonly start with high fissility intervals (DAD I or II) and become more massive towards to its top (DAD IV). The parasequences displayed at figure 13B are included in a transgressive sequence; consequently, each parasequence is more massive with respect to the older one.

XRD analysis, TOC and S1 pyrolysis results for each DAD class are presented in figure 14. According to fine-grained rock classification proposed by Passey *et al.* (2012), core intervals presenting high potential fissility are mainly siliceous mudstones whereas massive (*i.e.*, low fissility) rocks are mainly calcareous and mixed mudstones (Fig. 14A). A general characteristic of Vaca Muerta Formation rocks is its low percentage of clay (*e.g.,* Marchal *et al.*, 2018). XRD clay analysis shows a slight predominance of illite-smectite over the illite and kaolinite (Fig. 14B). The comparison of the XRD results with the DAD

index shows a clear correlation between low fissility classes and high carbonate content, no apparent relationship between fissility degree and clay content and mineralogy is found (Fig. 14A and B). In concordance with outcrop observations, the TOC values show a slight increase towards DAD classes with a high fissility potential (Fig. 14C). This trend becomes more conspicuous for the S1 average where the mode decreases towards the massive rocks (DAD IV) (Fig. 14D).

The relationship between DAD index classes and microscopic microfacies (Fig. 15) highlights the following trends:

(**i**) Rocks with high potential fissility (DAD I and II) correlate with silty and/or peloidal siliciclastic mudstones and occasionally calcareous bioclastic and silty mudstones. These microfacies exhibit the lowest values of carbonate and the highest percentage of silica, clay and pyrite according to XRD measurements.

(**ii**) Low fissility and massive rocks (DAD III and IV) corresponds to partially calcitized tuffs and microbial levels and, to a lesser extent, calcareous silty mudstones. These rocks display higher values of carbonate content and lower percentages of silica, clay and pyrite. Tuffs intensively replaced by carbonates and bindstones corresponds uniquely to the DAD class IV. Likewise, calcimetry measurements exhibit a similar relationship with higher values for DAD classes III and IV. Figure 16 shows an example of each DAD classes at both core and petrographic section with a description of their discontinuity planes.

Petrographic studies display a relationship between the matrix and the diagenetic processes that affect the rock and the DAD index: matrix in rocks that have high fissility potential are argillaceous or a mixture between siliceous, argillaceous and carbonatic. Rocks that tend to remain massive generally have a calcareous matrix (Fig. 16). Samples with evidence of matrix recrystallization or dolomitization are invariably massive (DAD IV).

Analysis of the DAD index regarding principal petrophysical parameters shows that rock samples corresponding to high potential fissility present low density and high porosity and permeability values. Massive and low fissility samples are characterized by higher densities and lower values of porosity and permeability (Fig. 17).
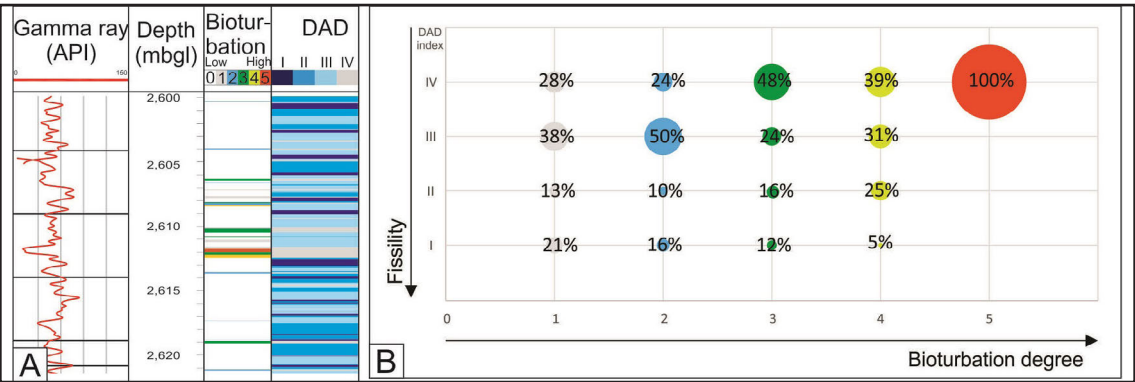
FIG 12. Fissility (DAD index) vs bioturbation degree (Lazar *et al.*, 2015). **A.** Detail from figure 10 displaying the strong relationship between highly bioturbated intervals (bioturbation index over 3) and massive rocks (DAD=IV). **B.** Percentage of bioturbation degree (1 to 5) for each DAD fissility index (I to IV). Note that most of the rocks correspond to relatively massive (DAD=III) to massive mudstones (DAD=IV), especially from bioturbation degree 3. Depth in meters below ground level (mbgl). The bioturbation index was extracted from Otharán (2020) and Otharán *et al.* (2022).
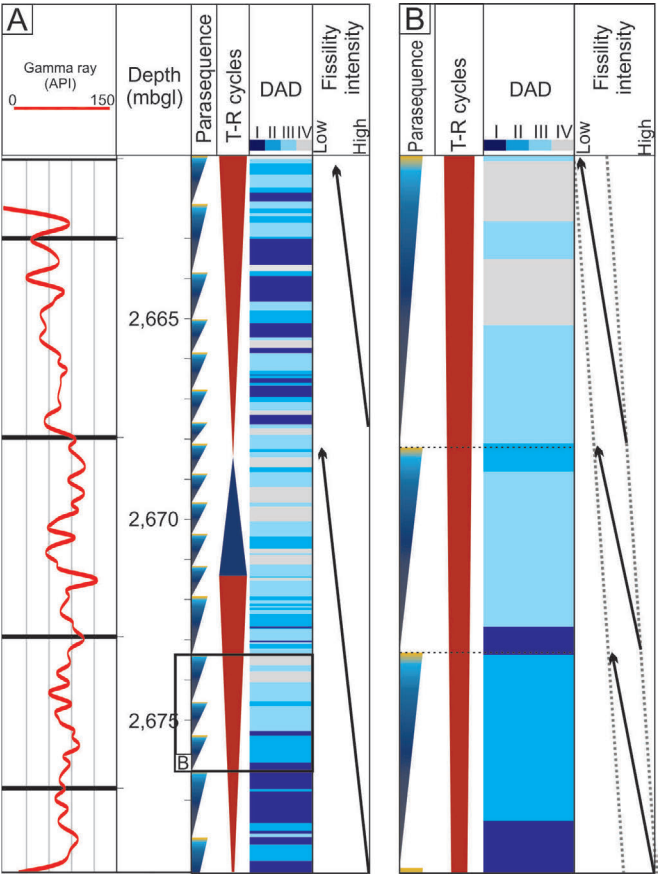
FIG 13. Relationship between fissility intensity (DAD index) and sequence stratigraphy. **A.** At Transgressive-Regressive (T-R) cycle scales. **B.** At parasequence scale. High fissility intensities (DAD=I or II) develop towards the first stages of the regressive system tracts and the bottom of the parasequences, which become less fissile (*i.e.*, more massive, DAD=III or IV) towards the top. Note that fissility intensity diminish between each parasequence towards the top. The sequential interpretation is based on Otharán (2020) and Otharán *et al.* (2022).
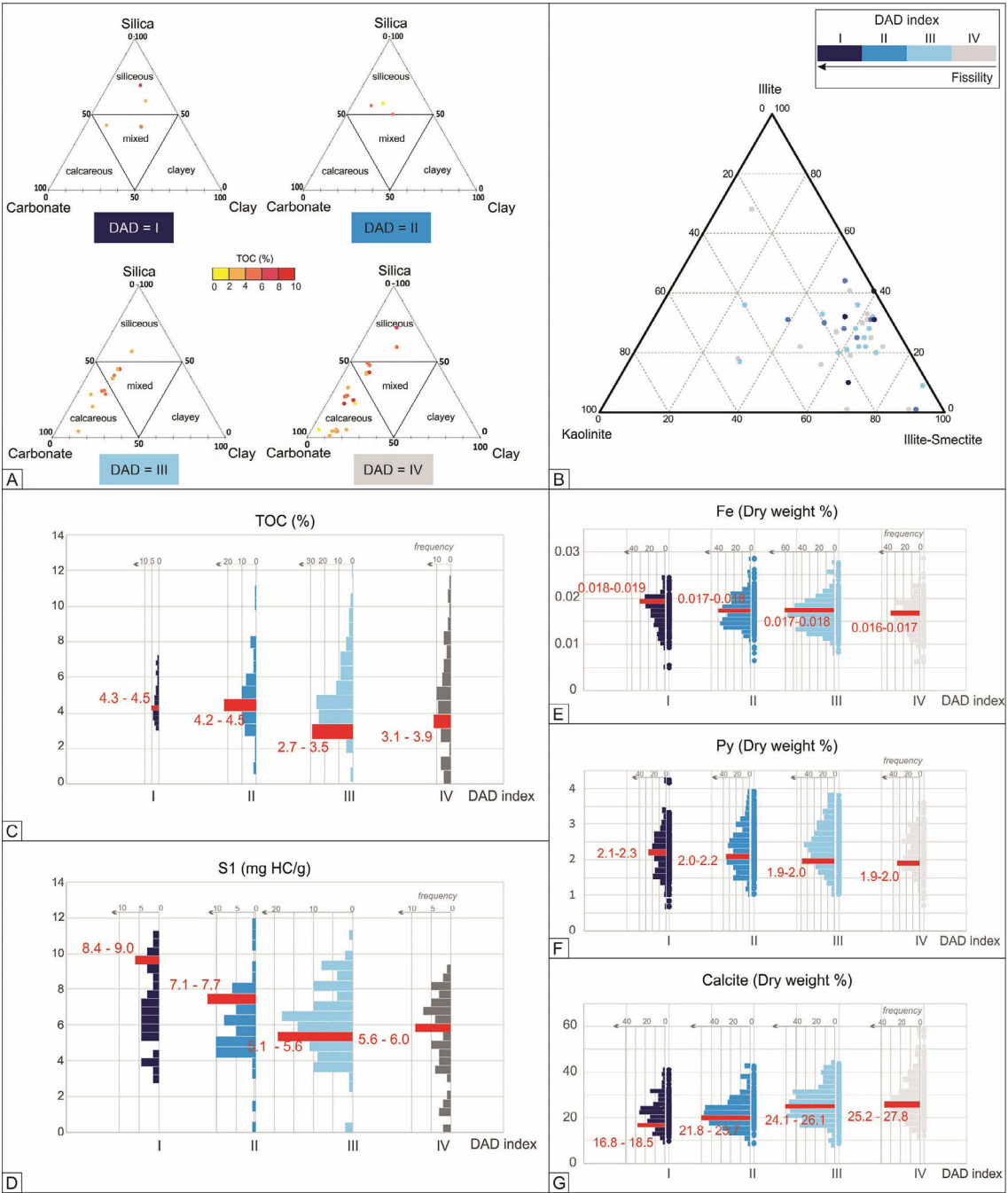
FIG 14. Results of DRX, pyrolysis analysis and mineralogical log. **A.** Ternary diagram showing Passey *et al.* (2012) mudstone rocks classification for each DAD class. **B.** Proportion of clay minerals in rocks of different fissility classes. **C.** TOC content. **D.** S1 values. Note that high fissility rocks show the higher organic matter content. **E.** Dry weight percentage of iron content. **F.** Dry weight percentage of pyrite content. **G.** Dry weight percentage of calcite. Histograms display mode interval values (in red) for each DAD class.
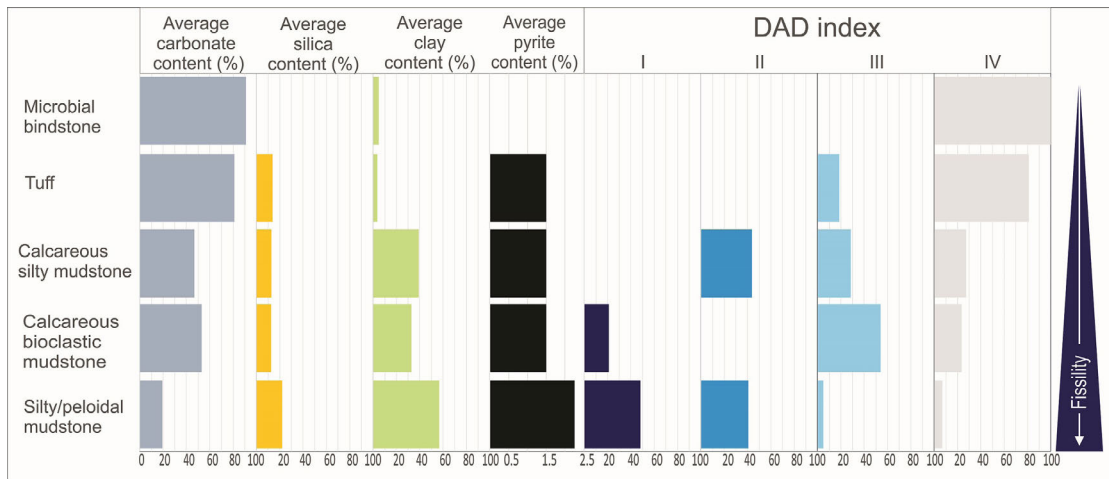
FIG 15. Microfacies identified at petrographic thin sections studies from the core samples indicating their average carbonate, silica, clay and pyrite DRX content and the proportion of DAD classes. Sillty/peloidal mudstones present the highest fissility and are characterized by low carbonate content and the highest values of silica, clay and pyrite content. In opposition, microbial bindstones are invariably massive and present the maximum carbonate content and the lowest values of silica, clay and pyrite content.

5.2.2. Well logs analysis

Figure 18A shows lamination density plotted against fissility density where dots are colored according to their DAD index. High lamination density rocks correlate with high fissility intervals, especially the first DAD class. In general, high fissility DAD classes (I and II) represent a narrow range of high lamination density values. Rocks with poor or none fissility (DAD III and IV) show a wide range of lamination density values reaching the lowest lamination density intervals, but also can include highly laminated rocks.

Porosity values compared with the DAD index (Fig. 18B) shows a positive correlation with fissility intensity: DAD class I shows mean porosity of 9.2% and a markedly unimodal distribution; DAD class II and III display lower porosity values (means of 8.3 and 7.6% respectively) and an incipient bimodal distribution; DAD class IV presents the lowest porosity values (mean of 7.5%) with a unimodal distribution.

The correlation between the mineralogical analysis and the DAD index shows key components related to the depositional environment (*e.g.,* redox conditions). The dry weight percentage of the iron (Fig. 14E) and pyrite (Fig. 14F) contents are higher for fissile rocks (DAD I and II) and decrease towards the massive intervals (DAD III and IV). Similar trends appear in the XRD pyrite content. The calcite content (Fig. 14G) shows an opposite behavior. Comparable

variations in the calcite content are also observed in outcrop and core.

The synthetic DAD index obtained from the supervised classification of the electric well logs reproduces the logged DAD index with a confidence between 60 and 70 % (Fig. 19A, B). DAD classes I and II intervals, representing high fissility rocks display high gamma ray values, narrow range of transit times and low values of photoelectric absorption factor and resistivity. In contrast, DAD classes III and IV intervals with poor or no fissility show low gamma ray responses, wide range of transition times and high values of photoelectric absorption factor and resistivity. Analysis of the crossplots in figure 19C shows that the resistivity log is the most important parameter to discriminate between all the DAD classes as it exhibits the widest dispersion. The shallow resistivity log is used in this model as a proxy for rock fabric, since it measures small variations at the first few millimeters of the borehole wall, similar to image logs (Linek *et al.*, 2007). This parameter is key for discrimination between DAD classes, highlightting the relevance of the textural control on fissility.

5.2.3. Geomechanical laboratory tests

The results of the geomechanical measurement tests of rock strength and stiffness show a good correlation with the DAD index (Fig. 20). Samples
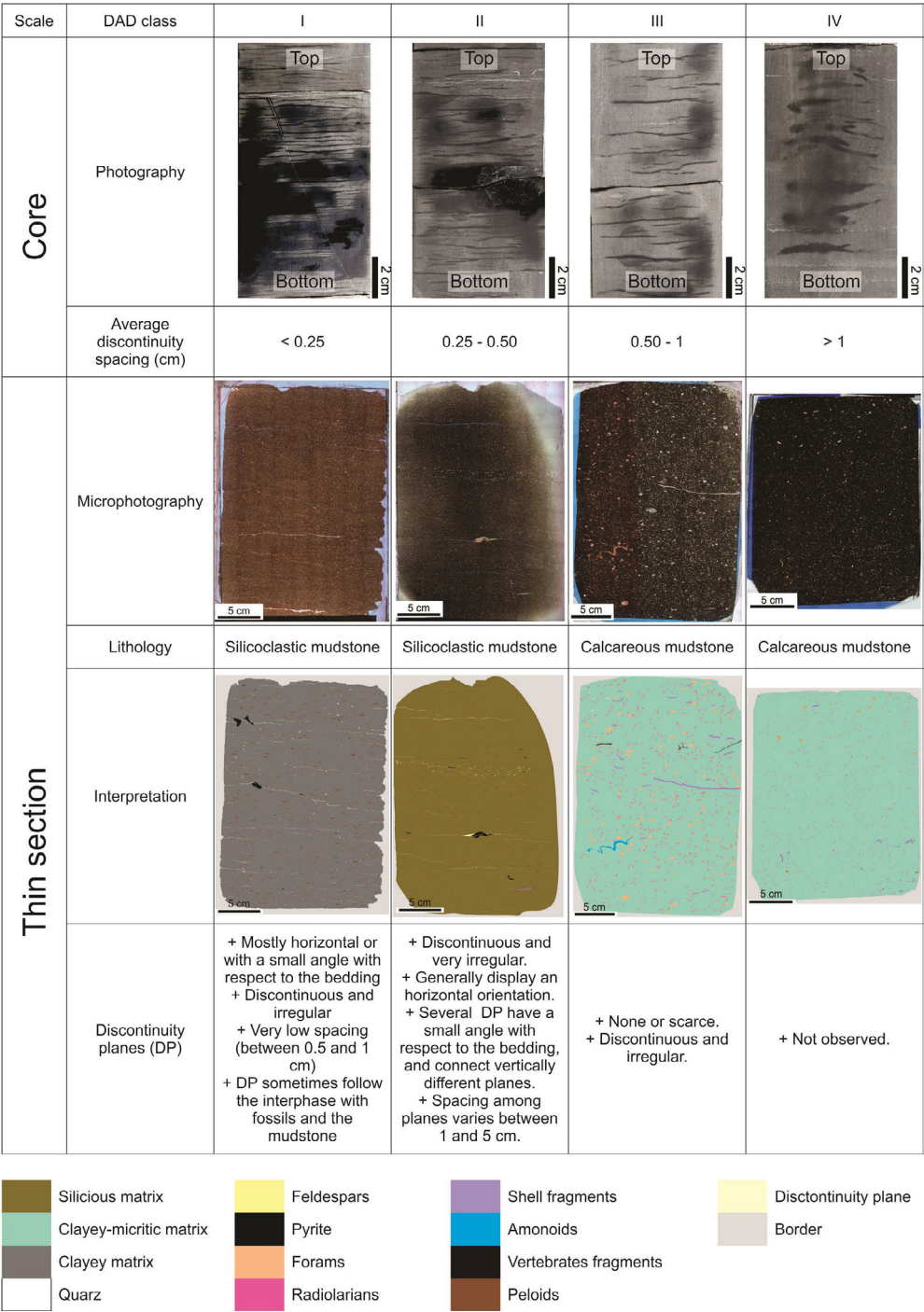
Scale	DAD class	I	II	III	IV
Core	Photography	Top ... Bottom (2 cm)	Top ... Bottom (2 cm)	Top ... Bottom (2 cm)	Top ... Bottom (2 cm)
	Average discontinuity spacing (cm)	< 0.25	0.25 - 0.50	0.50 - 1	> 1
Thin section	Microphotography	(5 cm)	(5 cm)	(5 cm)	(5 cm)
	Lithology	Silicoclastic mudstone	Silicoclastic mudstone	Calcareous mudstone	Calcareous mudstone
	Interpretation	(5 cm)	(5 cm)	(5 cm)	(5 cm)
	Discontinuity planes (DP)	+ Mostly horizontal or with a small angle with respect to the bedding + Discontinuous and irregular + Very low spacing (between 0.5 and 1 cm) + DP sometimes follow the interphase with fossils and the mudstone	+ Discontinuous and very irregular. + Generally display an horizontal orientation. + Several DP have a small angle with respect to the bedding, and connect vertically different planes. + Spacing among planes varies between 1 and 5 cm.	+ None or scarce. + Discontinuous and irregular.	+ Not observed.

Legend:
- Silicious matrix
- Clayey-micritic matrix
- Clayey matrix
- Quarz
- Feldespars
- Pyrite
- Forams
- Radiolarians
- Shell fragments
- Amonoids
- Vertebrates fragments
- Peloids
- Disctontinuity plane
- Border

FIG 16. DAD index displaying a representative example of each DAD class and the characteristics of the horizontal discontinuity planes interpreted as potential fissility planes. Note that both the average spacing between discontinuities at core sample and at petrographic thin sections are smaller in the case of DAD class I and II (high fissility intensity). In the case of the sample corresponding to the DAD class IV no discontinuities are observed. The matrix of low fissility to massive mudstones (DAD=III and IV) usually are calcareous, while those samples corresponding to high fissility intensity (DAD=I and II) normally exhibit a clayey, siliceous or mixed matrix.
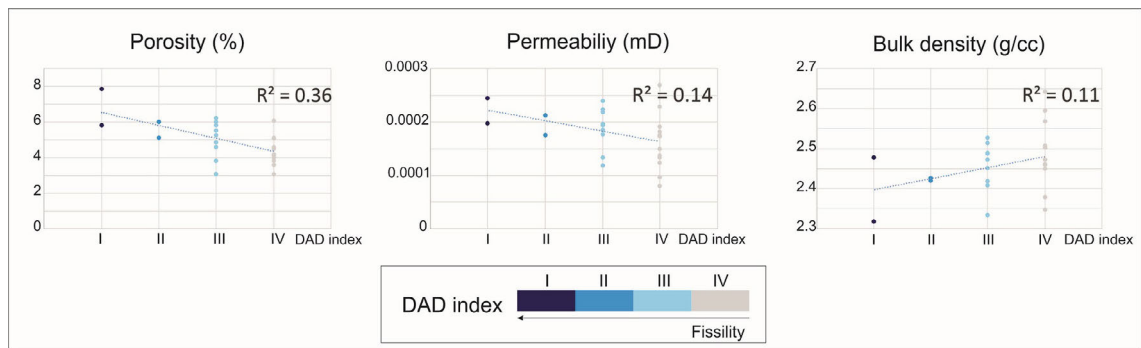
FIG 17. Petrophysical laboratory measurements regarding the different DAD classes, porosity, permeability and bulk density. High fissility rocks (DAD I and II) present higher porosity and permeability and lower bulk density values than their massive counterparts (DAD III and IV).
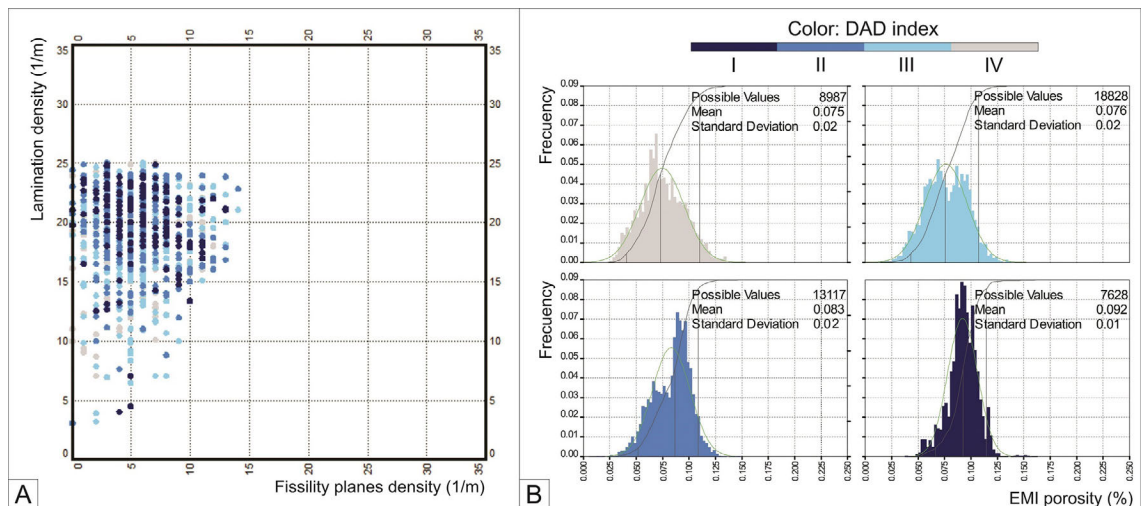

FIG 18. Electromagnetic interference image (EMI) analysis. **A.** Relationship between fissility (points colour according to DAD index), lamination density (vertical axis) and fissility planes density (horizontal axis). Note that high fissility intervals (dark blue points) correlate with high lamination density rocks. **B.** EMI porosity frequency histogram for each fissility class indicating their main statistical parameter. High fissility intervals (DAD=I and II) show higher porosity values than low fissility rocks (DAD=III and IV).

with low or no fissility have higher values of Young and Shear modulus and Poisson ratio than samples with high fissility (DAD I and II, Fig. 20A-C). The peak strength measurements performed parallel, perpendicular and at 45° degrees from bedding display an increase in strength towards DAD classes III and IV (Fig. 20D), implying that the rocks with a high fissility are the weakest.

Geomechanical laboratory measurements display a significant anisotropy in the studied rocks (Table 1 in Varela *et al.,* 2016), being horizontal plugs (parallel to the bedding) much stiffer than the vertical ones (perpendicular to the bedding). The anisotropy increases with fissility intensity (separation of the "v" and "h" trend lines, Fig. 20A-C). Both static and dynamic anisotropy parameters (ε and γ, Thomsen, 1986) show that high fissility rocks (DAD=II) are significantly more anisotropic than massive samples (DAD=IV). Even if most DAD class I rocks were undertested due to the difficulty to sample these highly fissile rocks, the few results obtained for this class confirm the general trends (Fig. 20).
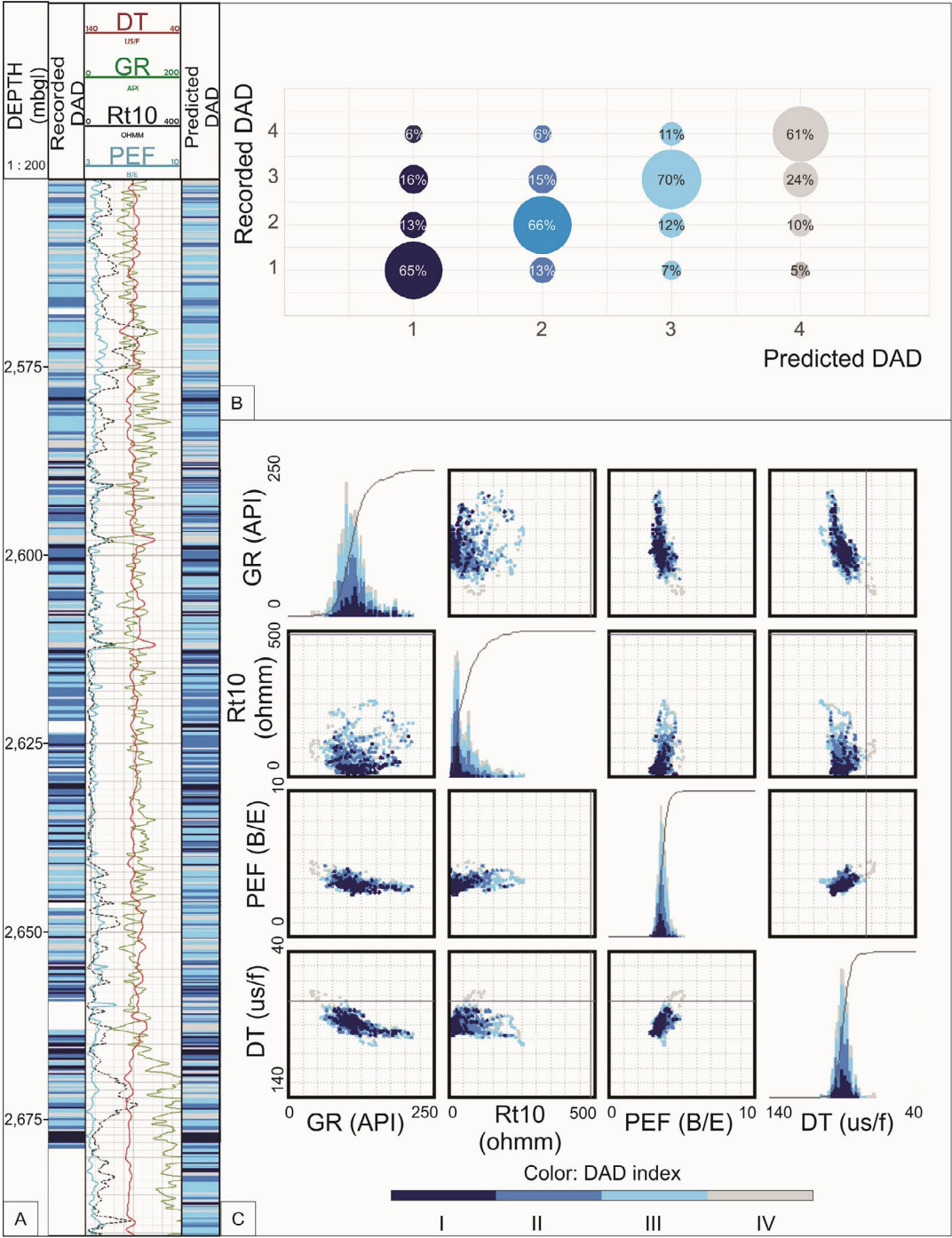
FIG 19. Comparison between synthetic and logged fissility (DAD) indexes in well A. **A.** Composite log displaying depth (track 1), measured DAD on the core (track 2), electric logs used in the supervised classification (track 3) and predicted DAD (track 4). **B.** Percentual correlation between the recorded DAD index and the DAD index predicted by the model. **C.** Cross plots of the electric log responses regarding the fissility (DAD) index. GR: gamma ray; RT10: shallow resistivity; PEF: photoelectric absorption factor; DT: sonic log. Note that the shallow resistivity (RT10) is the electric log with a wider dispersion among the crossplots, implying that it constitutes the best factor to discriminate between the DAD classes.
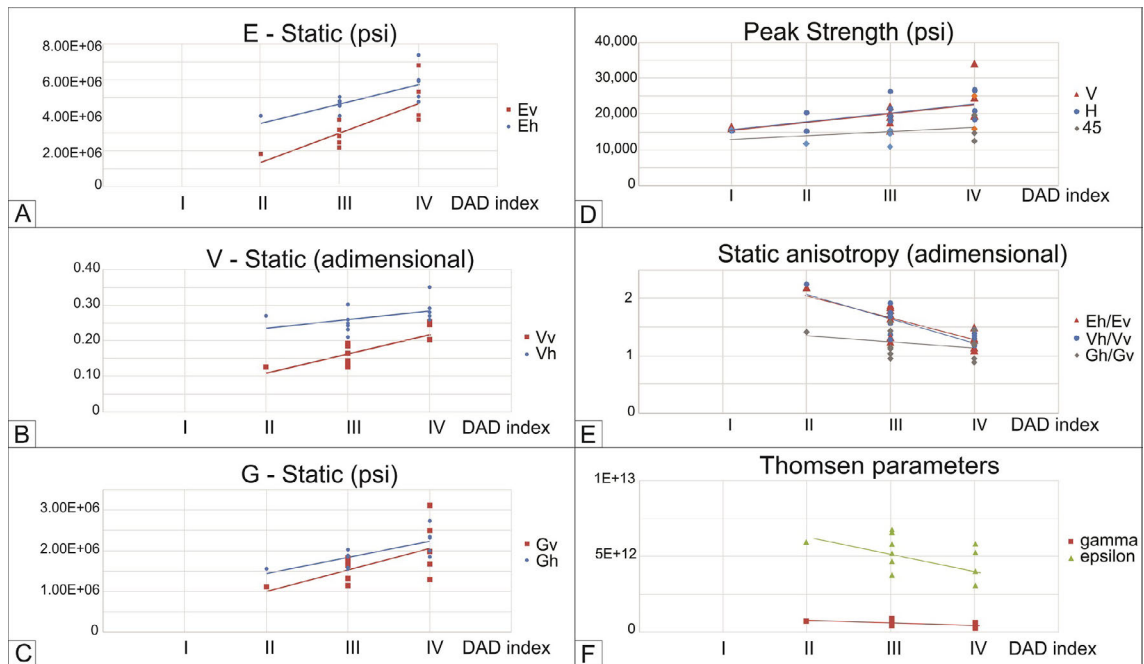
FIG 20. Geomechanical laboratory tests realized on the core samples: parameter results according to DAD index. **A.** E, static Young modulus. **B.** V, static Poisson ratio. **C.** G, static Shear modulus. **D.** Peak strength. **E.** Static anisotropy parameters. **F.** Anisotropy Thomsen parameters. For E, V, G, vertical (v) and horizontal (h) measurements and trend lines are displayed. For Peak Strength, additional 45° orientation is displayed.

6. Discussion

At the studied outcrop scale coexist both massive and fissile mudstones, suggesting inherited control on the rock response to weathering. This control is exerted by weakness planes that preexist underground and have been recognized in well core by the DAD methodology proposed in the present study. Numerous factors that depend both on depositional conditions and diagenetic processes control those second order discontinuities (Lewis, 1924; Ingram, 1953; O'Brien, 1970; Byers, 1974; Sintubin, 1994; Cripps and Czerewko, 2017).

6.1. DAD index

First order mechanical interfaces (*i.e.*, strong mechanical contrasts: contact of mudstones with concretions, tuffs and bed-parallel fractures) are weaker (Suarez-Rivera *et al.,* 2016) and less numerous than second order interfaces (*i.e.*, fossils imprints and fissility planes) since their relative proportion decreases from time T1 (31%) to T3 (21%) (Fig. 11B).

Part of these interfaces evolve into effective discontinuities related to core extraction processes such as core disking, (Jaeger and Cook, 1963) and anelastic strain recovery (gradual rock expansion over time, Blanton, 1983; Warpinski and Teufel, 1989). Both mechanisms result in discontinuities mostly parallel to stratification that tend to concentrate at the high fissility intervals through time (DAD I and II, Fig. 11A).

The evolution of potential into effective discontinuity planes (EDP) reveals the fissility in a subsurface (unmeteorized) rock (Fig. 10). EDP may develop by manipulation processes (*e.g.*, handling, slabbing) as well as decompression mechanisms through time: from T1 to T2 both mechanisms are involved whereas from T2 to T3 only the decompression is acting. The contrasting value of proportional increment between EDP associated with bed-parallel fractures (BPF) and the other discontinuities after five years of storage at atmospheric pressure and temperature (T3) can be explained by the low mechanical cohesion between BPF and the surrounding mudstone (Lee

et al., 2015), which causes those interfaces to split due to the differential pressure in core handling and slabbing (T2). Fissility planes are the most abundant anisotropies throughout the whole core over time, implying that fissility constitutes the most pervasive second order interface. The DAD index is a simple and accessible tool to estimate high fissility intervals in cored fine-grained rocks where the numerous fissility planes are not already effective discontinuities. This index shows a close relationship with mineralogical composition and organic matter content and texture characteristics, being the main controlling factors in fissility development (Fig. 21). Moreover, determining the fissility degree in unconventional reservoir rocks is key due to the influence in the mechanical behavior of the rock (see the following section 6.5).

6.2. Primary fissility controls

O'Brien (1970) stated that solely mudstones formed by the settling of individual particles could exhibit a very well-developed fissility, whereas rocks formed by flocculation only can achieve a low fissility degree. Clay flocculation may be promoted by absence or low content of iron oxides (Peterson, 1944; Ingram, 1953) and organic matter (Van Olphen, 1963; O'Brien, 1970). This inference is supported, in this work, by the slight decreasing trend in the iron content displayed by the chemical log (Fig. 14E) as

well as the small decreasing trend of the TOC and the S1 values shown by the pyrolysis result towards the massive intervals (Fig. 14C and D, respectively). These observations indicate the slight influence that flocculation may have on fissility development.

Fine-grained siliciclastic mudstones are prone to present a well-developed fissility whereas calcareous and mixed mudstones tend to be more massive. However, some of the calcareous mudstones develop good fissility (Figs. 8 and 16). In contrast, tuffs commonly replaced by carbonate and diagenetic calcareous levels are unequivocally massive (Figs. 10 and 15), with a DAD index of class IV. Thus, carbonate content is an important control on fissility development (Ingram, 1953). Carbonates present as bioclastic particles interrupt the parallel arrangement of platy particles, and, when present in the matrix as recrystallized micro-sparite and dolomite, the rocks tend to be massive. These trends are consistent with XRD and the mineralogical log values that indicate that massive rock intervals display higher carbonate content (Fig. 15), defining a relatively strong correlation between mudstone composition and fissility intensity (Fig. 21).

Spears, (1976) and Curtis *et al.* (1980) proposed that the primary control on fissility is related to the development of weakness planes at fine lamination interfaces. In agreement, mudstones with well-developed fissility and high lamination density
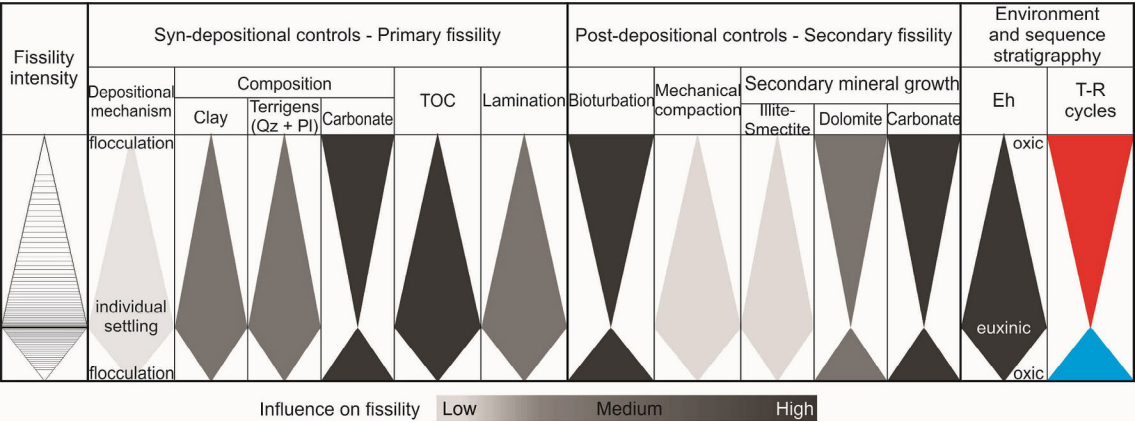

FIG. 21. Main factors controlling fissility development organized by depositional factors (inducing a primary fissility) and post-depositional factors (generating a secondary fissility). Based on our observations, the gray scale indicates the relevance that each factor has in the case of Vaca Muerta Formation rocks. In the case of the primary fissility, the main factors are the abundance of organic matter and carbonate content, while for the secondary fissility, the main controlling factors are the bioturbation and carbonatic pervasive diagenesis. Moreover, the environmental conditions and the sequential cycles related to each factor are indicated. Transgressive-Regressive (T-R) cycles represented in blue and red triangles, respectively.

are found both in outcrop (Fig. 7) and in well data (processed microresistivity images, Fig. 18). However, high lamination density values also occur in massive and poor fissility intervals, suggesting that it is not a unique factor. Furthermore, petrographic thin sections studies of rocks with a high fissility potential show that fine lamination does not always display horizontal discontinuity planes at the laminae interface. The effect of lamination in rocks of the Vaca Muerta Formation seems to be related to the cohesion between layers. Hence, the nature of the contacts is an important aspect to consider, as net contacts would exhibit a lower cohesion than the gradational contacts.

6.3. Secondary fissility controls

There is a strong correlation between moderate to high bioturbated rocks and massive intervals (DAD IV, Fig. 12). This observation is supported by XRD analysis where well-developed fissility rocks display higher pyrite content than their massive counterparts (Fig. 15). Pyrite is commonly used as an indicator of reducing conditions (Wilkin *et al.*, 1997; Wignall *et al.*, 2005; Zhou and Jiang, 2009), as it is stable only in suboxic to anoxic environments, where benthic live and bioturbation is scarce. The destruction of the syn-depositional structures by bioturbation and the resulting massiveness suggests that the rock fabric (and therefore, the subsequent fissility of the rock) is highly dependent on early stages of sediment lithification (Byers, 1974).

The role of mechanical compaction of sediments on fissility development was addressed by petrographic analyses. The parallel to bedding flattening of soft peloids (Figs. 8 and 16) does not appear to have a significant influence on rock fissility, since elongated peloids are present in massive and fissil mudstones. Although well A (Fig. 2) does not have information to evaluate clay fabric changes with depth, there is vast evidence that shows reorientations of platy components (clay minerals and organic matter particles) by mechanical compaction during the initial burial stages (O'Brien and Slatt, 1990; Sintubin, 1994; Alpin *et al.*, 2006). O'Brien and Slatt (1990) state that bedding oriented clay fabric generates during the first stages of burial, by a combination of overburden pressure and pore water expulsion, for tens of meters. Similarly, Sintubin (1994) suggests that a steady clay fabric develops once the clay particles have achieved a stable orientation distribution, which is no longer sensitive to overburden pressure, remaining unchanged during the subsequent burial history.

Studies on the diagenetic burial history of clay-rich sediments focus on the illitization of smectite, where transformation is mainly governed by temperature (*e.g.*, Pytte, 1989). Original phyllosilicate fabrics can be preserved to considerable burial depths (>5,000 m) before diagenesis imparts a preferred orientation (*e.g.*, Day-Stirrat *et al.*, 2008, 2011). If fissility is promoted by the parallel arrangement of platy minerals (*e.g.*, O'Brien and Slatt, 1990) and illite to smectite transformation favors a well-aligned phyllosilicates fabric, a high illite content should indicate a high fissility index (DAD I and II). The lack of correlation between the clay types and the DAD index (Fig. 14B) can be attributed to the incomplete illitization of the smectite at the studied interval of the core. Therefore, in this case the clay type and abundance cannot be used to track the fissilty, most probably related to the overall low clay content of the Vaca Muerta Formation rocks (Askenazi *et al.*, 2013; Marchal *et al.*, 2018; Spalletti *et al.*, 2019).

Bed-parallel fractures (BPF) are late diagenetic features (Rodrigues *et al.,* 2009), probably associated with fluid overpressure due to water release and hydrocarbon genesis within low-permeability source rocks (*e.g*., Cosgrove, 1995; Cobbold *et al.*, 2013; Gale *et al.*, 2014; Ravier *et al.*, 2020). Cerro Mulichinco outcrops of Vaca Muerta Formation contain one of the most abundant (~10% of the formation's volume, Rodrigues *et al.*, 2009), thickest, and most laterally continuous BPF in the world (Ukar *et al.*, 2020). Aditionally, in this site, numerous tectonic (non-bed parallel) fractures are also present due to the influence of the Agrio fold-and-thrust belt deformation (Valcarce *et al.*, 2006). The different fracture analysis existing at this location do not discriminate bed-parallel fractures from the rest, therefore an analysis of the vertical distribution of BPF was not possible. Ukar *et al.* (2020) observed that many BPF are localized at first order interfaces (carbonate concretions and tuffs-mudstone contact) and some at second-order interfaces (fossils-mudstone contacts). The relationship between fissility and BPF occurrence is variable in the studied core: the upper part of the core shows a positive correlation between high fissility and high BPF density, while towards the bottom of the core the relationship is negative. On the other hand, the distribution of the BPF in the Vaca Muerta Formation, both in outcrops (Rodrigues *et al.,* 2009;

Larmier, 2020; Ravier *et al.*, 2020) and subsurface (Domínguez *et al.*, 2016; Hernandez-Bilbao, 2016; Marchal *et al.*, 2016; Martínez *et al.*, 2017; Palacio *et al.*, 2018), shows an overall positive relationship with the TOC content, in which the base of the Vaca Muerta Formation (U1a, Figs. 2 and 9) displays the highest BPF frequency and the highest TOC (Fig. 10). Unfortunately, the main part of the basal unit of Vaca Muerta in well A is not cored (Fig.2). As shown previously, fissility has a positive correlation with TOC thus an overall positive correlation with bed-parallel fractures should be also expected. The variable correlation between fissility (second-order interfaces) and BPF (first-order interfaces) found by the DAD analysis scale could be originated by the nature of the interfaces. As shown previously (Fig. 11), first-order interfaces tend to convert in discontinuities prior to second order. Wang (2016) reported that about 75% of clear, mechanical interfaces were associated with BPV development in core.

6.4. Sequence stratigraphy and fissility

Core and detailed outcrop profile analysis show that high fissility mudrocks in the studied section of Vaca Muerta Formation, occur within the low energy environments. Low energy environments tend to contain more siliciclastic and finer grained material probably developed in less oxygenated waters, promoting the preservation (absence of bioturbation) of primary depositional features in the sediments and later on fissility development in the sedimentary rocks. Sequence stratigraphy analysis can be used for predicting the depositional environment and the rock fissility potential, as fissility intensity maintains a close relationship with the energy environment, at the transgressive-regressive cycles and at a parasequence scale in outcrop as well as in core data (Figs. 7 and 13). Fissility intensity is low in rocks formed at the beginning of the transgressive intervals, increases towards the maximum flooding surface and fades away at the end of the regressive intervals. At the parasequence scale, they usually begin with high fissility intensity that decreases towards the top (Fig. 13B). In general, the intervals of highest fissility develop near the maximum flooding surface at the peak of the transgressions, where an enrichment of organic matter occurs associated with terrigenous and clays inputs, depletion of carbonates (Kietzmann *et al.*, 2016) and bioturbation absence

(Almon *et al.*, 2002). According to Almon *et al.* (2002) and Kietzmann *et al.* (2016), an increase of the carbonate content together with a decrease of the terrigenous input is observed in the highstand system tracts of the Vaca Muerta Formation (Fig. 22). During the regressive periods, the carbonate ramp progrades towards the basin and the sediment exportation increases, promoting the dilution and oxidation of the organic matter (Hedges and Keil, 1995), increasing the proportion of equidimensional components and the benthonic organism's activity, giving rise to massive rocks (Fig. 21).

6.5. Petrophysical quality and geomechanical behaviour of the Vaca Muerta Formation sedimentary rocks

The positive correlation between fissility and porosity/permeability values (Fig. 17) relates with high organic matter content and large porosity values due to kerogen maturation (Sone and Zoback, 2013). Moreover, the slight increase in clay content within rock intervals with high fissility (Fig. 15) may be indicative of a relatively high porosity associated with pore space within clay minerals.

As all shale reservoirs, Vaca Muerta Formation rocks exhibit vertical transverse isotropy (VTI rock type: Thomsen, 1986; Ejofodomi *et al.*, 2014; Varela *et al.*, 2020) where the elastic parameter changes with the plug orientation with respect to bedding (*i.e.*, Ramos *et al.*, 2019; Sosa Massaro *et al.*, 2020), generating a variable anisotropy of the rocks. The studied rock samples characterized by high fissility index are more anisotropic than their massive counterparts (Fig. 20). Elastic anisotropy of fine-grained rocks is a function of their anisotropic fabric generated by the preferred orientation of platy minerals and the anisotropic elastic properties of the clay minerals (Sone and Zoback, 2013).

The Vaca Muerta Formation rocks with high fissility index are weaker (low elastic parameters, Fig. 20) than the massive mudstones due to their components and fabric. Sone and Zoback (2013) show that, in mudstones, the static and dynamic elastic parameters decrease with clay and kerogen content in the rocks since those are the most compliant constituents. However, due to sampling difficulties with highly fissile rocks, there could be a bias related to the low representation of DAD classes I and II both in the petrophysical and geomechanical measurements.
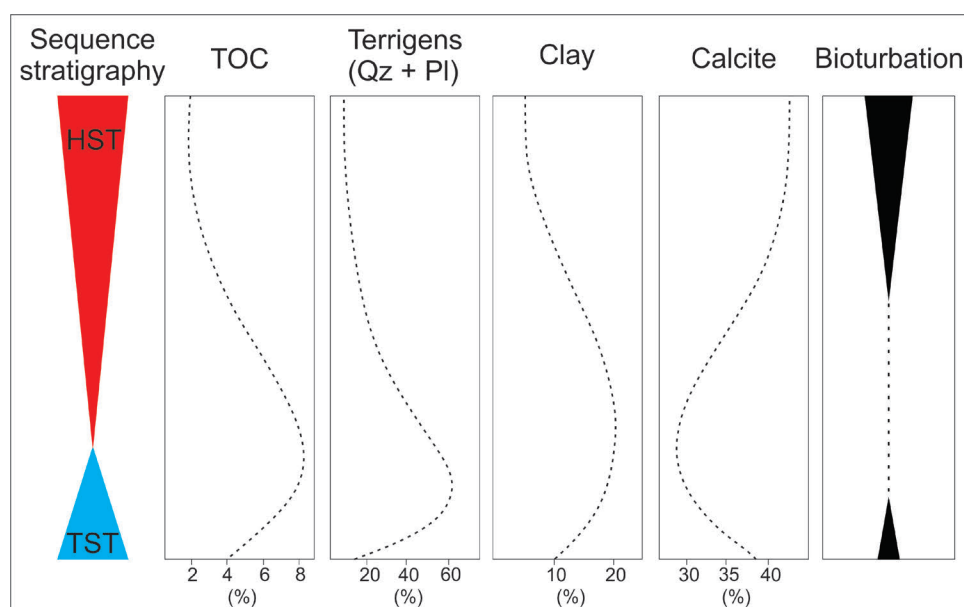
FIG. 22. Relationship between composition and transgressive (blue) -regressive (red) cycles observed at Vaca Muerta Formation. Modified from Almon *et al.* (2002) and Kietzmann *et al.* (2016). During the last periods of the Transgressive System Tract (TST), near the maximum flooding surface, the conditions for fissility development are the most favorable (high TOC, high terrigenous and clay input, low carbonate content and lack of bioturbation). Towards the end of the Highstand System Tracts (HST) the opposite conditions prompt massive and low fissile rock. Modified from Almon *et al*. (2002) and Kietzmann *et al*. (2016).

7. Conclusions

The present study proposes a new and straightforward methodology (DAD index) to estimate the degree of potential fissility of a cored fine-grained rock. This semi-quantitative methodology defines four fissility classes that can be predicted by using electrofacies generated from well logs that are frequently available in a well log set.

Among the parameters that contribute to fissility development, the rock composition, particularly the siliciclastic/carbonate ratio and TOC content, appear to be the most relevant. In the Vaca Muerta Formation highly fissile rocks display higher TOC, lower carbonate content and higher clay minerals participation than their massive counterparts. Furthermore, rock lamination can increase the fissility intensity, although not always the interfaces between different layers act as effective discontinuitiy planes.

The most favorable environmental conditions for enhancing rock fissility development in the studied core interval are associated with the maximum flooding surfaces, characterized by low carbonate, high clay minerals content and moderate to high TOC content.

Biologic processes, as bioturbation and variations of the carbonate content, generate important differences in the composition and rock fabric. Bindstones can be either massive or moderately fissil, depending on the biogenic components and clay participation. The correlation between massive intervals and highly bioturbated rocks allowed us to conclude that the fissility property is conditioned by syn-depositional and post-depositional processes from a very early stage of the burial history.

With respect to the petrophysical reservoir properties of Vaca Muerta Formation, the positive correlation between fissility and porosity/permeability values, indicate that high fissility intervals present a better petrophysical quality than those with none or poor fissility. These petrophysical properties are strongly related to the organic matter content. On the other hand, fissility increases the anisotropy of the rock, which also becomes more compliant, and may affect the efficiency of the hydraulic fracture treatment. The understanding of the generation mechanisms and the indirect prediction of this property can be beneficial for enhancing unconventional hydrocarbon production.

References

Ailing, H.L. 1945. Use of microlithologies as illustrated by some New York sedimentary rocks. Geological Society of America Bulletin 56 (7): 737-756.

Almon, W.R.; Dawson, W.C.; Sutton, S.J.; Ethridge, F.G.; Castelblanco, B. 2002. Sequence stratigraphy, facies variation and petrophysical properties in deepwater shales, Upper Cretaceous Lewis Shale, south-central Wyoming. Gulf Coast Association of Geological Societies Transactions 52: 1041-1053.

Alpin, A.C.; Matenaar, I.F.; McCarty, D.K.; van Der Pluijm, B.A. 2006. Influence of mechanical compaction and clay mineral diagenesis on the microfabric and pore-scale properties of deep-water Gulf of Mexico mudstones. Clays and Clay Minerals 54 (4): 500-514.

Askenazi, A.; Biscayart, P.; Cáneva, M.; Montenegro, S.; Moreno, M. 2013. Analogía entre la Formación Vaca Muerta y shale gas/oil plays de EEUU. *In* SPE Young Professional Committee: 1-20.

Bates, R.L.; Jackson, J.A. 1987. Glossary of Geology (3rd edition). American Geological Institute: 788 p. Alexandria, Virginia.

Bennett, R.H.; Bryant, W.R.; Hulbert, M.H. 1991. Microstructure of fine-grained sediments: From mud to shale. Springer Science and Business Media: 584 p. New York.

Berner, R.A.; Raiswell, R. 1983. Burial of organic carbon and pyrite sulfur in sediments over Phanerozoic time: a new theory. Geochimica et Cosmochimica Acta 47 (5): 855-862.

Blanton, T.L. 1983. The relation between recovery deformation and *in-situ* stress magnitudes. *In* SPE/DOE Low Permeability Gas Reservoirs Symposium, paper 11624: 213-218. Denver, Colorado.

Boitnott, G.; Louis, L.; Hampton, J.; Martinez, L.; Labeyrie, B.; Friry, I.; Lejay, A. 2018. High resolution geomechanical profiling in heterogeneous source rock from the Vaca Muerta Formation, Neuquén Basin, Argentina. *In* 52nd US Rock Mechanics/Geomechanics Symposium. American Rock Mechanics Association, ARMA 18-129: 8 p. Washington.

Burchette, T.P.; Wright, V.P. 1992. Carbonate ramp depositional systems. Sedimentary geology 79 (14): 3-57.

Byers, C.W. 1974. Shale fissility: relation to bioturbation. Sedimentology 21 (3): 479-484.

Campbell, G. 1946. New Albany Shale. Geological Society of America Bulletin 57 (9): 826-908.

Casala, S.; Palacios, J.; Vielma, J. 2019. Fracture Barrier Identification in Unconventional Formation Introducing a New Fracture Barrier Index from Conventional Logs: Vaca Muerta Case. *In* SPE Europec featured at 81st EAGE Conference and Exhibition. Society of Petroleum Engineers 3-6: SPE-195447-MS. London, UK.

Carozzi, A.V.; Orchuela, I.A.; Schelotto, M.R. 1993. Depositional Models of the Lower Cretaceous Quintuco-Loma Montosa Formation, Neuquén Basin, Argentina. Journal of Petroleum Geology 16 (4): 421-450.

Charpentier, D.; Worden, R.H.; Dillon, C.G.; Aplin, A.C. 2003. Fabric development and the smectite to illite transition in Gulf of Mexico mudstones: an image analysis approach. Journal of Geochemical Exploration 78: 459-463.

Cobbold, P.R.; Zanella, A.; Rodrigues, N.; Løseth, H. 2013. Bedding-parallel fibrous veins (beef and cone-in-cone): Worldwide occurrence and possible significance in terms of fluid overpressure, hydrocarbon generation and mineralization. Marine and Petroleum Geology 43: 1-20.

Cosgrove, J.W. 1995. The expression of hydraulic fracturing in rocks and sediments. Geological Society, Special Publications 92 (1): 187-196. London.

Cripps, J.C.; Czerewko, M.A. 2017. The influence of diagenetic and mineralogical factors on the breakdown and geotechnical properties of mudrocks. Geological Society, Special Publications 454 (1): 271-293. London

Curtis, C.D.; Lipshie, S.R.; Oertel, G.; Pearson, M.J. 1980. Clay orientation in some Upper Carboniferous mudrocks, its relationship to quartz content and some inferences about fissility, porosity and compactional history. Sedimentology 27 (3): 333-339.

Day-Stirrat, R.J.; Alpin, A.C.; Sroron, J.; Van der Pluijm, B.A. 2008. Diagenetic reorientation of phyllosilicate minerals in Paleogene mudstones of the Podhale Basin, southern Poland. Clays and minerals 56 (1): 100-111.

Day-Stirrat, R.J.; Dutton, S.P.; Milliken, K.L.; Loucks, R.G.; Aplin, A.C.; Hillier, S.; van der Pluijm, B.A. 2010.

Fabric anisotropy induced by primary depositional variations in the silt: clay ratio in two fine-grained slope fan complexes: Texas Gulf Coast and northern North Sea. Sedimentary Geology 226 (1-4): 42-53.

Day-Stirrat, R.J.; Schleicher, A.M.; Schneider, J.; Flemings, P.B.; Germaine, J.T.; van der Plujim, B.A. 2011. Preferred orientation of phyllosilicates: Effects of composition and stress on resedimented mudstone microfabrics. Jounal of Structural Geology 33(9): 1347-1358.

Dewhurst, D.N.; Siggins, A.F.; Sarout, J.; Raven, M.D.; Nordgård-Bolås, H.M. 2011. Geomechanical and ultrasonic characterization of a Norwegian Sea shale. Geophysics 76 (3): WA101-WA111.

Desjardins, P.; Fantín, M.; González Tomassini, F.; Reijenstein, H.; Sattler, F.; Domínguez, F.; Kietzmann, D.; Leanza, H.; Bande, A.; Benoit, S.; Borgnia, M.; Vittore, F.; Simo, T.; Minisini, D. 2016. Estratigrafía Sísmica Regional. *In* Transecta Regional de la Formación Vaca Muerta Integración de sísmica, registros de pozos, coronas y afloramientos (González, G.; Vallejo, D.; Desjardins, P.; González-Tomassini, F.; Kietzmann, D.; Rivarola, L.; Domínguez, F.; editors). Instituto Argentino de Petróleo y del Gas: 5-22. Buenos Aires.

Domínguez, R.F.; Lanusse Noguera, I.; Continanzia, M.J.; Mykietiuk, K.; Ponce, C.; Pérez, G.; Guerello, R. 2016. Organic-rich stratigraphic units in the Vaca Muerta Formation and their distribution and characterization in the Neuquén Basin (Argentina). *In* Unconventional Resources Technology Conference, 1-3:1439-1450. San Antonio, Texas.

Domínguez, R.F.; Reijenstein, H.; Kohler, G.; Sattler, F.; Moreno, M.J.; Rivarola, L.G.; Borgnia, M. 2017. Distribución regional de quiebres de clinoformas del sistema Vaca Muerta-Quintuco. *In* Congreso Geológico Argentino, No. 20, Vol. 5: 7-11. San Miguel de Tucumán.

Doveton, J.H. 1994. Multivariate Pattern Recognition and Classification Methods. *In* Geologic Log Analysis Using Computer Methods. American Association of Petroleum Geologists (AAPG), Computer Application in Geology Vol 2: 65-95.

Dunham, R.J. 1962. Classification of carbonate rocks according to depositional textures. American Association of Petroleum Geologists (AAPG), Memoir 1: 108-121.

Ejofodomi, E.A.; Varela, R.A.; Cavazzoli, G.; Velez, E.I.; Peano, J. 2014. Development of an optimized completion strategy in the Vaca Muerta Shale with an anisotropic geomechanical model. European Unconventional Conference and Exhibition, SPE 167806: 25-27. Vienna, Austria.

Fawad, M.; Mondol, N.H.; Jahren, J.; Bjørlykke, K. 2010. Microfabric and rock properties of experimentally compressed silt-clay mixtures. Marine and Petroleum Geology 27 (8): 1698-1712.

Gale, J.F.; Laubach, S.E.; Olson, J.E.; Eichhubl, P.; Fall, A. 2014. Natural fractures in shale: A review and new observations Natural Fractures in Shale: A Review and New Observations. AAPG Bulletin 98 (11): 2165-2216.

Garcia, M.N.; Sorenson, F.; Bonapace, J.C.; Motta, F.; Bajuk, C.; Stockman, H. 2013. Vaca muerta shale reservoir characterization and description: the starting point for development of a shale play with very good possibilities for a successful project. *In* Unconventional Resources Technology Conference (URTeC), Society of Exploration Geophysicists, American Association of Petroleum Geologists, Society of Petroleum Engineers. Paper 1508336: 863-899. Denver, Colorado.

Geikie, A. 1903. Text-book of Geology. Macmillan and Company: 680 p. London.

Giambiagi, L.; Bechis, F.; Lanés, S.; Tunik, M.; García, V.; Suriano, J.; Mescua, J. 2008. Formación y evolución triásico-jurásica del Depocentro Atuel, Cuenca Neuquina, provincia de Mendoza. Revista de la Asociación Geológica Argentina 63: 520-533.

Gipson, M. 1965. Application of the electron microscope to the study of particle orientation and fissility in shale. Journal of Sedimentary Research 35 (2): 408-414.

González-Tomassini, F.; Hryb, D.; Palacio, J.P.; Lazzari, V.; Bertoldi, F.; Sagasti, G. 2017. Caracterización e impacto de las heterogeneidades identificadas en subsuelo en la Formación Vaca Muerta. *In* Congreso Geológico Argentino, No. 20, Simposio Geología de la Formación Vaca Muerta, Vol. 67: 67-71. San Miguel de Tucumán.

Grabau, A.W. 1913. Principles of stratigraphy. AG Seiler and Co.: 1185 p. New York.

Grim, R.E.; Cuthbert, F.L. 1945. Some Clay-Water Properties of Certain Clay Minerals. Journal of the American Ceramic Society 28 (3): 90-95.

Gulisano, C.A.; Gutiérrez Pleimling, A.R.; Digregorio, R.E. 1984. Análisis estratigráfico del intervalo Tithoniano-Valanginiano (Formaciones Vaca Muerta, Quintuco y Mulichinco) en el suroeste de la provincia de Neuquén. *In* Congreso Geológico Argentino, No. 9, Actas 1: 221-235. San Carlos de Bariloche.

Hedges, J.I.; Keil, R.G. 1995. Sedimentary organic matter preservation: an assessment and speculative synthesis. Marine chemistry 49 (2-3): 81-115.

Hernandez-Bilbao, E. 2016. High-resolution chemo-stratigraphy, sequence stratigraphic correlation, porosity and fracture characterization of the Vaca Muerta Formation, Neuquén Basin, Argentina, Ph.D. Thesis (Unpublished) dissertation, Colorado School of Mines: 195 p.

Ho, N.C.; Peacor, D.R.; van der Pluijm, B.A. 1999. Preferred orientation of phyllosilicates in Gulf Coast mudstones and relation to the smectite-illite transition. Clays and Clay Minerals 47 (4): 495-504.

Howell, J.A.; Schwarz, E.; Spalletti, L.A.; Veiga, G.D. 2005. The Neuquén Basin: an overview. *In* The Neuquén Basin, Argentina: A Case Study in Sequence Stratigraphy and Basin Dynamics. *In* Geological Society, Special Publications (Veiga, G.D.; Spalletti, L.A.; Howell, J. A.; Schwarz, E.; editors) 252: 1-14. London.

Hurst, C.W. 1987. Post-depositional structural changes in clay sediments. Ph.D. Thesis (Unpublished), Sheffield City Polytechnic: 174 p.

Ilgen, A.G.; Heath, J.E.; Akkutlu, I.Y.; Bryndzia, L.T.; Cole, D.R.; Kharaka, Y.K.; Kneafsey, T.J.; Milliken, K.L.; Pyrak-Nolte, L.J.; Suarez-Rivera, R. 2017. Shales at all scales: Exploring coupled processes in mudrocks. Earth-Science Reviews 166: 132-152.

Ingram, R.L. 1953. Fissility of mudrocks. Geological Society of America Bulletin 64 (8): 869-878.

Jaeger, J.C.; Cook, N.G.W. 1963. Pinching-off and disking of rocks. Journal of Geophysical Research 68 (6): 1759-1765.

Keller, W.D. 1946. Evidence of texture on the origin of the Cheltenham fireclay of Missouri and associated shales. Journal of Sedimentary Research 16 (2): 63-71.

Kerr, P.F. 1937. Attapulgus clay. American Mineralogist: Journal of Earth and Planetary Materials 22 (5): 534-550.

Kietzmann, D.A.; Palma, R.M.; Bressan, G.S. 2008. Facies y microfacies de la rampa tithoniana-berriasiana de la Cuenca Neuquina (Formación Vaca Muerta) en la sección del Arroyo Loncoche-Malargüe, provincia de Mendoza. Revista de la Asociación Geológica Argentina 63 (4): 696- 713.

Kietzmann, D.A.; Palma, R.M.; Riccardi, A.C.; Martín-Chivelet, J.; López-Gómez, J. 2014. Sedimentology and sequence stratigraphy of a Tithonian-Valanginian carbonate ramp (Vaca Muerta Formation): a misunderstood exceptional source rock in the Southern Mendoza area of the Neuquén Basin, Argentina. Sedimentary Geology 302: 64-86.

Kietzmann, D.A.; Ambrosio, A.L.; Suriano, J.; Alonso, M.S.; Tomassini, F.G.; Depine, G.; Repol, D. 2016. The Vaca Muerta-Quintuco system (Tithonian-Valanginian) in the Neuquén Basin, Argentina: A view from the outcrops in the Chos Malal fold and thrust belt. AAPG Bulletin 100 (5): 743-771.

Kietzmann, D.A.; Llanos, M.P.I.; Palacio, J.P.; Sturlesi, M.A. 2021. Facies analysis and stratigraphy across the Jurassic-Cretaceous boundary in a new basinal Tithonian-Berriasian section of the Vaca Muerta Formation, Las Tapaderas, Southern Mendoza Andes, Argentina. Journal of South American Earth Sciences (109): 103267. doi: 10.1016/j.jsames.2021.103267.

King, G.E. 2010. Thirty years of gas shale fracturing: What have we learned? *In* SPE Annual Technical Conference and Exhibition. Paper 133456: 1-50. Florence, Italy.

Krim, N.; Bonnel, C.; Tribovillard, N.; Imbert, P.; Aubourg, C.; Riboulleau, A.; Fasentieux, B. 2017. Paleoenvironmental evolution of the southern Neuquén basin (Argentina) during the Tithonian-Berriasian (Vaca Muerta and Picún Leufú Formations): a multi-proxy approach. Bulletin de la Société Géologique de France 188 (5): 1-33.

Krumbein, W.C. 1947. Shales and their environmental significance. Journal of Sedimentary Research 17 (3): 101-108.

Larmier, S. 2020. Génération de fluides, migration et fracturation au sein des roches mères: cas de la formation de la Vaca Muerta, bassin de Neuquén, Argentine. Hydrologie. Université du Maine: 545 p.

Lash, G.G.; Blood, D.R. 2004. Origin of shale fabric by mechanical compaction of flocculated clay: evidence from the Upper Devonian Rhinestreet Shale, western New York, USA. Journal of Sedimentary Research 74 (1): 110-116.

Lazar, O.R.; Bohacs, K.M.; Macquaker, J.H.; Schieber, J.; Demko, T.M. 2015. Capturing key attributes of fine-grained sedimentary rocks in outcrops, cores, and thin sections: nomenclature and description guidelines. Journal of Sedimentary Research 85 (3): 230-246.

Lazzari, V.; Hryb, D.; Manceda, R.; Foster, M. 2015. Predicción de fracturas naturales en la Fm Vaca Muerta. Petrotecnia 56 (1): 64-77.

Lee, H.P.; Olson, J.E.; Holder, J.; Gale, J.F.; Myers, R.D. 2015. The interaction of propagating opening mode fractures with pre existing discontinuities in shale. Journal of Geophysical Research: Solid Earth 120 (1): 169-181.

Legarreta, L.; Gulisano, C. 1989. Análisis estratigráfico secuencial de la Cuenca Neuquina (Triásico superior-Terciario inferior). *In* Cuencas Sedimentarias Argentinas, Serie Correlación Geológica (Chebli, G.; Spalletti, L.A.; editors). Universidad Nacional de Tucumán: 221-243. San Miguel de Tucumán.

Legarreta, L.; Uliana, M.A. 1991. Jurassic-Cretaceous marine oscillations and geometry of back-arc basin fill, central Argentine Andes. In International Association of Sedimentology, Special Publication 12: 429-450.

Legarreta, L.; Uliana, M.A. 1996. The Jurassic Succession in West-central Argentina: Stratal Patterns, Sequences

and Paleogeographic Evolution. Paleogeography, Paleoclimatology and Paleoecology 120: 303-330.

Legarreta, L. 2002. Eventos de desecación en la Cuenca Neuquina: depósitos continentales y distribución de hidrocarburos. *In* Congreso de Exploración y Desarrollo de Hidrocarburos, No 5, Trabajos Técnicos, Actas en CD, Mar del Plata.

Legarreta, L.; Villar, H.J. 2012. Las facies generadoras de hidrocarburos de la Cuenca Neuquina. Petrotecnia 53 (4): 14-39.

Legarreta, L.; Villar, H.J. 2015. The Vaca Muerta Formation (Late Jurassic-Early Cretaceous), Neuquén Basin, Argentina: Sequences, Facies and Source Rock Characteristics. *In* Unconventional Resources Technology Conference, Society of Exploration Geophysicists, American Association of Petroleum Geologists, Society of Petroleum Engineers, Extended Abstract, URTeC: 2170906. San Antonio, Texas.

Lejay, A.; Larmier, S.; Rutman, P.; Gelin, F. 2017. The role of porosity in the development of parallel bedded calcite filled fractures (or beef) in the Vaca Muerta: an integrated analysis from high resolution core data. In Unconventional Resources Technology Conference, Society of Exploration Geophysicists, American Association of Petroleum Geologists, Society of Petroleum Engineers: 394-409. Austin, Texas.

Lewis, J.V. 1924. Fissility of Shale and Its Relations to Petroleum. Bulletin of the Geological Society of America 35 (3): 557-590.

Linek, M.; Jungmann, M.; Berlage, T.; Pechnig, R., Clauser, C. 2007. Rock classification based on resistivity patterns in electrical borehole wall images. Journal of Geophysics and Engineering 4 (2): 171-183.

Lundegard, P.D.; Samuels, N.D. 1980. Field classification of fine-grained sedimentary rocks. Journal of Sedimentary Research 50 (3): 781-786.

Macdonald, D.; Gómez Pérez, I.; Franzese, J.; Spalletti, L.; Lawver, L.; Gahagan, L.; Dalziel, I.; Thomas, C.; Trewin, N.; Hole, M.; Paton, D. 2003. Mesozoic break-up of SW Gondwana: implications for regional hydrocarbon potential of the southern South Atlantic. Marine and Petroleum Geology 20: 287-308.

Manceda, R.; Figueroa, D. 1993. La inversión del rift mesozoico de la faja fallada y plegada de Malargüe, Provincia de Mendoza. *In* Congreso Geológico Argentino, No. 12, Actas 3: 219-232.

Marchal, D.; Sattler, F.; Köhler, G. 2016. Sierra Chata. *In* Transecta Regional de la Formación Vaca Muerta Integración de sísmica, registros de pozos, coronas y afloramientos (González, G.; Vallejo, D.; Desjardins, P.; González-Tomassini, F.; Kietzmann, D.; Rivarola,

L.; Domínguez, F.; editors). Instituto Argentino de Petróleo y del Gas: 155-167. Buenos Aires.

Marchal, D.; González, G.; Domínguez, F. 2018. Mineralogic analysis of the Vaca Muerta Formation. *In* Regional Cross Section of the Vaca Muerta Formation: Integration of seismic, well logs, cores and outcrops. (González, G.; Vallejo, M.D.; Kietzmann, D.; Marchal, D.; Desjardins, P.; González-Tomassini, F.; Gómez Rivarola, L.; Domínguez, R.F.; editors) Special Publication of Instituto Argentino del Petróleo y del Gas (IAPG): 33-44. Buenos Aires.

Marchal, D.; Manceda, R.; Domínguez, R.D.; Sattler, F. 2020. Structural geology: Tectonic history, macrostructures, regional fault map, fault systems, second-order structures, and impact of the inheritance. *In* Integrated geology of unconventionals: The case of the Vaca Muerta play, Argentina (Minisini, D.; Fantín, M.; Lanusse Noguera, I.; Leanza, H.A.; editors). The American Association of Petroleum Geologists (AAPG) Memoir 121: 99-140. Tulsa, Oklahoma.

Martínez, V.; Musso, T.; Pettinari, G.; Molina, A. 2017. Litofacies, mineralogía y caracterización de microfracturas naturales (venillas rellenas de calcita tipo beef) en el intervalo basal de la Formación Vaca Muerta en el Bajo de Añelo, Cuenca Neuquina. *In* Congreso Geológico Argentino, No. 20, Simposio Geología de la Formación Vaca Muerta, Actas (85): 85-90. San Miguel de Tucumán.

Minisini, D.; Eldrett, J.; Bergman, S.C.; Forkner, R. 2017. Chronostratigraphic framework and depositional environments in the organic-rich, mudstone-dominated Eagle Ford Group, Texas, USA. Sedimentology 65 (5): 1520-1557.

Minisini, D.; Fryklund, B.; Gerali, F.; Fantín, M. 2020. The first economical unconventional play outside North America: Context, history, and "coopetition". *In* Integrated Geology of Unconventionals: The Case of the Vaca Muerta Play, Argentina (Minisini, D.; Fantín, M.; Lanusse Noguera, I.; Leanza, H.A; editors). The American Association of Petroleum Geologists (AAPG) 121: 1-24. Tulsa, Oklahoma.

Mitchum, R.M.; Uliana, M.A. 1985. Seismic stratigraphy of carbonate depositional sequences, Upper JurassicLower Cretaceous, Neuquén Basin, Argentina. *In* Seismic Stratigraphy, II: an Integrated Approach to Hydrocarbon Exploration (Berg, O.; Woolverton, D.; editors). American Association of Petroleum Geologist Memoirs 39: 255-274.

Mohr, E.C.J.; Pendleton, R.L. 1944. Soils of equatorial regions with special reference to the Netherlands East Indies. Edwards Brothers, Inc.: 766 p. Amsterdam.

Mosquera, A.; Silvestro, J.; Ramos, V.; Alarcón, M.; Zubiri, M. 2011. La estructura de la Dorsal de Huincul. *In* Congreso Geológico Argentino, No. 8, Actas: 385-397. San Luis.

Mpodozis, C.; Kay, S. 1990. Provincias magmáticas ácidas y evolución tectónica de Gondwana: Andes chilenos (28-31°S). Revista Geológica de Chile 17 (2): 153-180.

Mutti, E.; Gulisano, C.A.; Legarreta, L. 1994. Anomalous systems tracts stacking patterns within third order depositional sequences (Jurassic-Cretaceous Back Arc Neuquén Basin, Argentine Andes). *In* Second High-Resolution Sequence Stratigraphy Conference, Abstract Book (Posamentier, H.W.; Mutti, E.; editors), International Union of Geological Sciences (IUGS) 137-143. Tremp.

O'Brien, N.R. 1970. The fabric of shale-an electron-microscope study. Sedimentology 15 (3-4): 229-246.

O'Brien, N.R.; Slatt, R.M. 1990. Argillaceous rock atlas. Springer-Verlag: 141 p. New York.

Odom, I.E. 1967. Clay fabric and its relation to structural properties in mid-continent Pennsylvanian sediments. Journal of Sedimentary Research 37 (2): 610-623.

Olarte, M.C.; Ruge, J.C. 2020. Analysis of the relationship between water retention curve, particle size distribution and the pore size distribution in the characterization of a collapsible porous clay. Respuestas 25 (1): 33-43.

Otharán, G. 2020. Sedimentología y análisis de facies de la Formación Vaca Muerta (Tithoniano-Valanginiano), Cuenca Neuquina. El rol de los flujos de fango en la depositación de espesas sucesiones de lutitas (Ph.D Thesis). Universidad Nacional del Sur: 422 p. Bahía Blanca,

Otharán, G.; Zavala, C.; Arcuri, M.; Di Meglio, M.; Zorzano, A.; Marchal, D.; Köhler, G. 2020. Análisis de facies en depósitos de grano fino asociados a flujos de fango. Formación Vaca Muerta (Tithoniano-Valanginiano), Cuenca Neuquina central, Argentina. Andean Geology 47 (2): 384-417. doi: 10.5027/andgeoV47n2-3061.

Otharán, G.; Zavala, C.; Marchal, D.; Köhler, G. 2022. Sedimentología y análisis de facies de alta resolución en testigos corona de la Formación Vaca Muerta, Cuenca Neuquina, Argentina. *In* Congreso Geológico Argentino, No. 21, 4: 959–960. Puerto Madryn.

Ortiz, A.C.; Hryb, D.E.; Martínez, J.R.; Varela, R.A. 2016. Hydraulic fracture height estimation in an unconventional vertical well in the vaca muerta formation, neuquen basin, argentina. *In* SPE Hydraulic Fracturing Technology Conference, Society of Petroleum Engineers, SPE-179145-MS. Texas.

Palacio, J.P.; Hryb, D.E.; González-Tomassini, F. 2018. Predicción de la distribución de beefs en la Formación Vaca Muerta: Un análisis integrado. *In* Congreso de Exploración y Desarrollo de Hidrocarburos, No. 10, Simposio de Recursos No Convencionales, paper: 181-192. Mendoza.

Passey, Q.R.; Bohacs, K.M.; Esch, W.L.; Klimentidis, R.; Sinha, S. 2012. My source rock is now my reservoir-Geologic and petrophysical characterization of shale-gas reservoirs. AAPG Search and Discovery Article, 80231:1-47.

Payne, T.G. 1942. Stratigraphical analysis and environmental reconstruction. American Association of Petroleum Geologists (AAPG) Bulletin 26 (11): 1697-1770.

Peterson, J.E. 1944. The effect of montmorillonitic and kaolinitic clays on the formation of platy structures. Soil Science Society of America Proceedings 9 (C): 37-48.

Pettijohn, F.J. 1975. Sedimentary rocks, 3rd edition. Harper & Row: 628 p. New York.

Pirsson, L.V. 1920. A Text-Book of Geology for use in Universities: Physical Geology (Part 1), John Wiley & Sons, 2dn editoin: 283 p. New York.

Potter, P.E.; Maynard, J.B.; Depetris, P.J. 2005. Mud and mudstones: Introduction and overview. Springer Science & Business Media: 297 p. Würzburg.

Pytte, A.M.; Reynolds, R.C. 1989. The thermal transformation of smectite to illite. *In* Thermal history of sedimentary basins (Naeser, N.D.; McCulloh, T.H.; editors). Springer-Verlag: 133-140. New York.

Ramos, M.J.; Espinoza, D.N.; Laubach, S.E.; Torres-Verdín, C. 2019. Quantifying static and dynamic stiffness anisotropy and nonlinearity in finely laminated shales: Experimental measurement and modeling. Geophysics 84 (1): 25-36.

Ramos, V.A. 1999. Evolución tectónica de la Argentina. *In* Geología Argentina Servicio Geológico Minero Argentino (Caminos, R.; editor). Anales 29: 715-784. Buenos Aires.

Ramos, V.A. 2010. The tectonic regime along the Andes: present-day and Mesozoic regimes. Geological Journal 45: 2-25.

Ramos, V.A.; Folguera, A. 2005. Tectonic evolution of the Andes of Neuquén: constraints derived from the magmatic arc and Foreland deformation. *In* The Neuquén Basin, Argentina: A Case Study in Sequence Stratigraphy and Basin Dynamics (Veiga, G.D.; Spalletti, L.A.; Howell, J.A.; Schwarz, E.; editors), Geological Society of London, Special Publication: 15-35. London.

Ramos, V.A.; Naipauer, M.; Leanza, H.A.; Sigismondi, M.E. 2020. The Vaca Muerta Formation of the Neuquén Basin: An Exceptional Setting along the

Andean Continental Margin. *In* Integrated geology of unconventionals: The case of the Vaca Muerta play, Argentina (Minisini, D.; Fantín, M.; Lanusse Noguera, I.; Leanza, H.A.; editors), The American Association of Petroleum Geologists (AAPG) Memoir 121: 25-37. Tulsa, Oklahoma.

Ravier, E.; Martinez, M.; Pellenard, P.; Zanella, A.; Tupinier, L. 2020. The milankovitch fingerprint on the distribution and thickness of bedding-parallel veins (beef) in source rocks. Marine and Petroleum Geology 122: 104643. 10.1016/j.marpetgeo.2020.104643.

Rezaee, R. 2015. Fundamentals of Gas Shale Reservoirs. John Wiley & Sons, Inc.: 399 p. Hoboken, New Jersey.

Rodrígues, N.; Cobbold, P.R.; Løseth, H.; Ruffet, G. 2009. Widespread bedding-parallel veins of fibrous calcite ("beef") in a mature source rock (Vaca Muerta Fm., Neuquén Basin, Argentina): evidence for overpressure and horizontal compression. Journal of the Geological Society 166: 695-709.

Rodríguez-Blanco, L.; Eberli, G.P.; Weger, R.J.; McNeill, D.F.; Swart, P.K. 2022. Quantifying concretion distribution in shales of the Vaca Muerta-Quintuco system, Neuquén Basin, Argentina. American Association of Petroleum Geologists (AAPG) Bulletin 106 (2): 409-436. doi: 10.1306/08182120059.

Rosenqvist, I.T. 1966. Norwegian research into the properties of quick clay-a review. Engineering Geology 1 (6): 445-450.

Sagasti, G.; Foster, M.; Hryb, D.; Ortiz, A.; Lazzari, V. 2014. Understanding geological heterogeneity to customize field development: An example from the Vaca Muerta unconventional play, Argentina. *In* Unconventional Resources Technology Conference (URTeC), Society of Exploration Geophysicists, American Association of Petroleum Geologists, Society of Petroleum Engineers: 797-816. Denver, Colorado.

Sattler, F.; Domínguez, R.F.; Fantín, M.; Desjardins, P.; Reijenstein, H.; Benoit, S.; Borgnia, M.; Vittore, F.; González Tomassini, F.; Feinstein, E.; Kietzmann, D.; Marchal, D. 2016. *In* Transecta Regional de la Formación Vaca Muerta Integración de sísmica, registros de pozos, coronas y afloramientos (González, G.; Vallejo, D.; Desjardins, P.; González-Tomassini, F.; Kietzmann, D.; Rivarola, L.; Domínguez, F.; editors). Instituto Argentino de Petróleo y del Gas, Anexo 1: 5-22. Buenos Aires.

Sintubin, M. 1994. Clay fabrics in relation to the burial history of shales. Sedimentology 41 (6): 1161-1169.

Slatt, R.M. 2011. Important geological properties of unconventional resource shales. Central European Journal of Geosciences 3 (4): 435-448.

Sone, H.; Zoback, M.D. 2013. Mechanical properties of shale-gas reservoir rocks-Part 1: Static and dynamic elastic properties and anisotropy. Geophysics 78 (5): D381-D392.

Sosa Massaro, A.P.; Espinoza, D.N.; Benitez, P.E.; Frydman, M. 2020. Vaca Muerta Formation: From Laboratory Geomechanical Characterization to the Unconventional Reservoir Application. *In* US Rock Mechanics/Geomechanics Symposium, No. 54, American Rock Mechanics Association (ARMA) 1649: 3730-3738. Golden, Colorado.

Spalletti, L.A.; Franzese, J.R.; Matheos, S.D.; Schwarz, E. 2000. Sequence stratigraphy of a tidally dominated carbonate-siliciclastic ramp; the Tithonian-Early Berriasian of the Southern Neuquén Basin, Argentina. Journal of the Geological Society 157: 433-446.

Spalletti, L.A.; Remírez, M.N.; Sagasti, G. 2019. Geochemistry of aggradational-Progradational sequence sets of the Upper Jurassic-Lower Cretaceous Vaca Muerta shales (Añelo area, Neuquén Basin, Argentina): Relation to changes in accommodation and marine anoxia. Journal of South American Earth Sciences 93: 495-509.

Spears, D.A. 1976. The fissility of some Carboniferous shales. Sedimentology 23 (5): 721-725.

Stinco, L.P.; Barredo, S.P. 2014. Vaca muerta formation: An example of shale heterogeneities controlling hydrocarbon accumulations. *In* Unconventional Resources Technology Conference (URTec), Society of Exploration Geophysicists, American Association of Petroleum Geologists, Society of Petroleum Engineers: 2854-2868. Denver, Colorado.

Suarez-Rivera, R.; Von Gontent, W.D.; Graham, J.; Ali, S.; Degenhardt, J.; Jegadeesan, A. 2016. Optimizing lateral landing depth for improved well production. *In* Unconventional Resources Technology Conference, No. 4, Proceedings: URTeC-2460515. San Antonio, Texas.

Thomsen, L. 1986. Weak Elastic Anisotropy. Geophysics 51 (10): 1954-1966.

Twenhofel, W.H. 1936. Terminology of the fine grained mechanical sediments. National Research Council, Division of Geology and Geography 5: 81-104.

Twenhofel, W.H. 1939. Environments of origin of black shales. American Association of Petroleum Geologists (AAPG) Bulletin 28 (8): 1178-1198.

Ukar, E.; López, R.G.; Gale, J.F.W.; Laubach, S.E.; Manceda, R. 2017. New type of kinematic indicator in bed-parallel veins, Late Jurassic-Early Cretaceous Vaca Muerta Formation, Argentina: E-W shortening during Late Cretaceous vein opening. Journal of Structural Geology 104: 31-47.

Ukar, E.; López, R.G.; Hryb, D.; Gale, J.F.W.; Manceda, R.; Fall, A.; Brisson, I.; Hernandez-Bilbao, E.; Weger, R.J.; Marchal, D.A.; Zanella, A.; Cobbold, P.R. 2020. Natural fractures: From core and outcrop observations to subsurface models. *In* Integrated geology of unconventionals: The case of the Vaca Muerta play, Argentina (Minisini, D.; Fantín, M.; Lanusse Noguera, I.; Leanza, H.A.; editors). The American Association of Petroleum Geologists (AAPG) Memoir 121: 377-416. Tulsa, Oklahoma.

Uliana, M.; Biddle, K. 1988. Mesozoic-Cenozoic paleogeographic and geodynamic evolution of Southern South America. Revista Brasileira de Geociências 18 (2): 172-190.

Uliana, M.A.; Legarreta, L. 1993. Hydrocarbons habitat in a Triassic-to-Cretaceous sub-Andean setting: Neuquén Basin, Argentina. Journal of Petroleum Geology 16 (4): 397-420.

Valcarce, G.Z.; Zapata, T.; del Pino, D.; Ansa, A. 2006. Structural evolution and magmatic characteristics of the Agrio fold-and-thrust belt. Special Papers-Geological Society of America 407: 125-145.

Van Olphen, H. 1963. An lntroduction to Clay Colloid Chemistry. Interscience-Wiley: 301 p. New York.

Varela, R.A.; Marchal, D.; Perez Mazas, A.M.; Porras, Sattler, J.F.; Cavazzoli, G.; Lagarrigue, E. 2016. Integrated geomechanical characterization for Vaca Muerta Formation: Shale oil well integration from logs, core and pressures for fracture optimization: 50th US Rock Mechanics/Geomechanics Symposium, ARMA-2016-095. Houston, Texas.

Varela, R.A.; Marchal, D.; Cuervo, S.; Lombardo, E.F.; Perl, Y.P.; Hryb, D.E.; Pateti, P.; Nielsen, O. 2020. Geomechanics: Pressure, stress field, and hydraulic fractures. *In* Integrated geology of unconventionals: The case of the Vaca Muerta play, Argentina (Minisini, D.; Fantín, M.; Lanusse Noguera, I.; Leanza, H.A.; editors), The American Association of Petroleum Geologists (AAPG) Memoir 121: 351-376. Tulsa, Oklahoma.

Vergani, G.D.; Tankard, A.J.; Belotti, H.J.; Welkink, H.J. 1995. Tectonic evolution and paleogeography of the Neuquén Basin, Argentina. *In* Petroleum Basins of South America (Tankard, A.J.; Suárez Soruco, R.; Welsink, H.J.; editors). The American Association of Petroleum Geologists (AAPG) Memoir 62: 383-402. USA.

Vernik, L.; Milovac, J. 2011. Rock physics of organic shales. The Leading Edge 30 (3): 318-323.

Walton, I.; McLennan, J. 2013. The role of natural fractures in shale gas production. ISRM international conference for effective and sustainable hydraulic fracturing. International Society for Rock Mechanics and Rock Engineering: 327-356. Brisbane, Australia.

Wang, Q. 2016. Characterization of bedding-parallel fractures in shale: Morphology, size distribution and spatial organization. Doctoral dissertation, University of Texas: 295 p.

Warpinski, N.R.; Teufel, L.W. 1989. A Viscoelastic Constitutive Model for Determining *in-Situ* stress magnitudes from anelastic strain recovery of core. SPE production engineering 4 (3): 272-280.

Weaver, C. 1931. Paleontology of the Jurassic and Cretaceous of west-central Argentina. University of Washington Memoirs 1: 1-595.

Weller, J.M. 1930. Cyclical sedimentation of the Pennsylvanian Period and its significance. The Journal of Geology 38 (2): 97-135.

White, W.A. 1961. Colloid phenomena in sedimentation of argillaceous rocks. Journal of Sedimentary Research 31 (4): 560-570.

Wignall, P.B.; Newton, R.; Brookfield, M.E. 2005. Pyrite framboid evidence for oxygen-poor deposition during the Permian-Triassic crisis in Kashmir. Palaeogeography, Palaeoclimatology, Palaeoecology 216 (3-4): 183-188.

Wilkin, R.T.; Arthur, M.A.; Dean, W.E. 1997. History of water-column anoxia in the Black Sea indicated by pyrite framboid size distributions. Earth and Planetary Science Letters 148 (3-4): 517-525.

Xing, P.; Suárez-Rivera, R.; Dontsov, E. 2020. Induced fracturing during Coring and core retrieval in unconventional reservoirs. *In* US Rock Mechanics/Geomechanics Symposium, No. 54. American Rock Mechanics Association (ARMA) 20-1970. Houston, Texas.

Yrigoyen, M.R. 1991. Hydrocarbon resources of Argentina. Petrotecnia. *In* World Petroleum Congress, No. 13, Special Issue: 38-54. Buenos Aires.

Zavala, C.; Arcuri, M.; Di Meglio, M.; Zorzano, A.; Otharán, G. 2015. Proyecto Vaca Muerta, Informe Final. Petrobras unpublished report: 295 p.

Zhou, C.; Jiang, S.Y. 2009. Palaeoceanographic redox environments for the lower Cambrian Hetang Formation in South China: Evidence from pyrite framboids, redox sensitive trace elements, and sponge biota occurrence. Palaeogeography, Palaeoclimatology, Palaeoecology 271 (3-4): 279-286.